

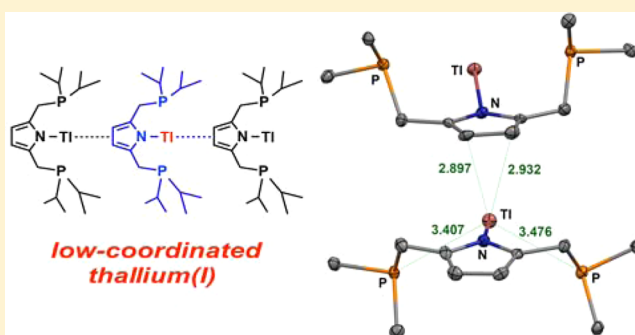
Ag(I) and Tl(I) Precursors as Transfer Agents of a Pyrrole-Based Pincer Ligand to Late Transition Metals

Julie A. Kessler and Vlad M. Iluc*

Department of Chemistry and Biochemistry, University of Notre Dame, 251 Nieuwland Science Hall, Notre Dame, Indiana 46556, United States

Supporting Information

ABSTRACT: A PNP ligand, $\text{PN}^{\text{Pyr}}\text{P}$ ($(\text{PN}^{\text{Pyr}}\text{P})\text{H} = 2,5$ -bis((di-*iso*-propylphosphino)methyl)pyrrole), which employs a pyrrole unit as a central anionic nitrogen donor, was designed. The corresponding group 10 metal chlorides as well as iridium and ruthenium compounds were isolated. In order to conduct this work, $[(\text{PN}^{\text{Pyr}}\text{P})\text{Tl}]$ and $[(\text{PN}^{\text{Pyr}}\text{P})\text{Ag}]_2$ were synthesized and characterized. The thallium and silver species were paramount in the formation of the iridium and ruthenium complexes, which could not be isolated using $(\text{PN}^{\text{Pyr}}\text{P})\text{H}$ or the corresponding lithium pyrrolide salt. Interestingly, the solid state molecular structure of $[(\text{PN}^{\text{Pyr}}\text{P})\text{Tl}]$ indicates that the metal center engages in an η^2 intermolecular interaction with the backbone of a neighboring pyrrole molecule instead of the expected bonding to the phosphine arms.



INTRODUCTION

Pincer ligands have become an indisputable means to create stable, reactive, and easily tunable transition metal catalysts.^{1–7} In particular, PNP systems are well studied and known to facilitate a variety of catalytic transformations depending on the transition metal center.^{4–8} The central nitrogen donor of these ligands can be either neutral or anionic.^{5,7–9} The use of a pyrrole unit as the central donor has been studied,^{10–20} but a corresponding tridentate PNP system has been reported only recently.^{21–24}

We became interested in the synthesis of iridium and ruthenium metal complexes supported by a pyrrole-based PNP because of the proven utility of these metals in catalytic cycles.^{7,25–29} Iridium was the metal of choice due to the well-established ability of iridium pincer complexes to perform efficiently in small molecule activation and hydrogenation reactions.^{30–33} In the early stages of this research, it became evident that the pyrrole N–H bond would not add oxidatively to the iridium center, as has been shown to occur with other protonated PNP ligands,³⁴ thus requiring multiple means of deprotonation and transmetalation to be investigated. The synthesis of $(\text{PN}^{\text{Pyr}}\text{P})\text{H}$ (2,5-bis((di-*iso*-propylphosphino)methyl)-1*H*-pyrrole), its metalation to silver and thallium, and the corresponding transmetalation reactions yielding iridium, ruthenium, nickel, palladium, and platinum complexes are described here. Additionally, a comparison between the formation of these late transition-metal complexes from the pro-ligand, the lithium pyrrolide salt, and the silver and thallium analogues will be discussed.

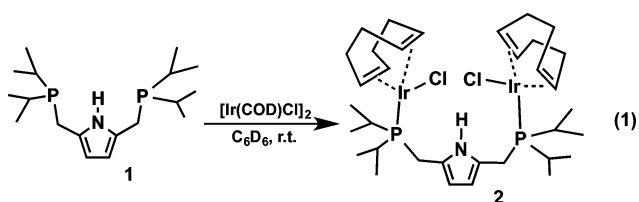
RESULTS AND DISCUSSIONS

Direct metalation. The pro-ligand $(\text{PN}^{\text{Pyr}}\text{P})\text{H}$ (**1**) was synthesized similarly to recent reports of analogues containing phenyl or cyclohexyl substituted phosphine donors.^{21–24} The use of *iso*-propyl substituents on phosphines was advantageous due to low cost, high solubility in common organic solvents, and ease of identification by NMR spectroscopy. The formation of an iridium pincer with a monoanionic PNP framework, $[(\text{PNP})\text{Ir}(\text{H})(\text{Cl})]$ (PNP = bis(2-di-*iso*-propylphosphino)-4-methylphenylamide) by oxidative addition of the N–H bond to iridium was reported to occur at ambient conditions.³⁴ However, this result does not apply to the present PNP-pyrrole system. Reactions between the pro-ligand, $(\text{PN}^{\text{Pyr}}\text{P})\text{H}$, and 0.5 equiv of $[\text{Ir}(\text{COD})\text{Cl}]_2$ were conducted in C_6D_6 and monitored by NMR spectroscopy, and a mixture of products was observed. Different solvents and varying temperatures were explored. The cleanest result was achieved by cooling a tetrahydrofuran solution of $(\text{PN}^{\text{Pyr}}\text{P})\text{H}$ to -78 °C and adding the iridium starting material at this low temperature before allowing it to reach room temperature. The crude mixture of this reaction contained unreacted free ligand and a bimetallic species, $[(\text{PN}^{\text{Pyr}}\text{P})\text{H}\{\text{Ir}(\text{COD})\text{Cl}\}_2]$ (**2**, eq 1), which was crystallographically characterized (Figure 1). The $^{31}\text{P}\{\text{H}\}$ NMR spectrum of **2** indicates a single resonance at 20.06 ppm, suggesting that other metalation attempts (see below) might also have yielded this bimetallic species.

Compound **2** is structurally similar to a rhodium complex recently synthesized by Goldman et al.³⁵ From the reaction of

Received: July 4, 2014

Published: November 11, 2014



^tBu₂furPOP (2,5-bis((di-*tert*-butylphosphino)methyl)furan) with [Rh(NBD)Cl]₂ (NBD = norbornadiene), a bimetallic product was obtained, (μ-(^tBu₂furPOP)[Rh(NBD)Cl]₂), in which each rhodium atom coordinates to a phosphine donor, NBD, and a chloride. This bimetallic rhodium species was also an unanticipated reaction product.

It became evident that additional steps must be taken in order to achieve tridentate coordination of the PN^{PP}P anion; thus, the use of a deprotonating agent was investigated. ⁿBuLi was used originally, as it is a viable means to create a lithium pyrrolide species,²¹ from which LiCl precipitation would occur together with N–Ir bond formation upon the addition of [Ir(COD)Cl]₂. However, ³¹P{¹H} NMR spectra from these reactions show many resonances, including a septet at –1 ppm, possibly indicating a complex/oligomeric network consisting of Li–P interactions,³⁶ which are associated with complicated ¹H NMR spectra. The lithium pyrrolide [(PN^{PP}P)Li] (3) was generated and used *in situ* but could also be isolated by recrystallization from a hexanes solution as an off-white powder in poor yield. Its ³¹P{¹H} NMR spectrum contained a septet at –1.01 ppm (C₆D₆), while the ⁷Li spectrum contained a pentet (2.50 ppm, C₆D₆) with a *J*_{P–Li} coupling constant of 25 Hz. These splitting patterns indicate that each phosphorus atom couples equally to two lithium atoms, and each lithium atom couples equally to four phosphorus atoms. A dimeric structure is likely, based on spectroscopic similarities to other lithiated organophosphorus compounds.^{36–39}

Since formation of an iridium complex containing the anionic PN^{PP}P ligand was not observed from reactions with either the pro-ligand or the lithium-pyrrolide, 3 was combined with [(DME)NiCl₂] to prove its viability as a precursor. Consistent

with other reported observations,²¹ [(PN^{PP}P)NiCl] (4) was formed quickly, cleanly, and in good yield (78%). Compound 4 was structurally characterized (Figure 2) and has similar metrical parameters to the analogous pyrrole-based species [NiCl(P₂^{Ph}Pyr)]²³ and [NiCl(P₂^{Cy}Pyr)].²⁴

The ¹H NMR spectrum of 4 contains two sets of apparent quartets for the *iso*-propyl methine groups (12H each), one multiplet for the *iso*-propyl methylene protons (4H), a virtual triplet for the methylene protons (4H), and a singlet for the pyrrole backbone (2H). The splitting of the methylene protons into a virtual triplet has been previously described^{22,23,40} and is explained by the meridional coordination of the ligand, in which the methylene protons couple to equivalent phosphines (singlet resonance at 60.53 in the ³¹P{¹H} NMR spectrum). Virtual triplets are also observed in the corresponding ¹³C{¹H} NMR spectrum for the methine, methylene, and pyrrole-tertiary carbons for the same reason.

Because of the successful formation of 4 from 3, the analogous syntheses of [(PN^{PP}P)PdCl] (5) and [(PN^{PP}P)PtCl] (6) were also attempted. Complex 5 could be isolated as a red solid in a moderate yield (66%) upon filtration from a toluene solution, while 6 was observed (52%) among a mixture of products and could not be recrystallized from the reaction mixture.

Since these group 10 metal complexes (4–6) could be obtained from the lithium pyrrolide reagent, their formation from the pro-ligand was also pursued (Scheme 2). Upon mixing 1 and [(DME)NiCl₂] in tetrahydrofuran, the solution became orange and 4 could be isolated in good yield (79%). However, reactions of 1 with [(COD)PdCl₂] and [(COD)PtCl₂] did not lead to the desired products. We hypothesize that the Pd-containing product is a dimer similar to that observed by Mani, [Pd₂Cl₄{μ-C₄H₃N-2,5-(CH₂PPh₂)₂-κ²-PP₂}]₂ in the reaction between 2,5-bis(diphenylphosphinomethyl)pyrrole and [PdCl₂(PhCN)₂];²² no major Pt-containing product was identified in the reaction mixture, which was mainly unreacted free ligand.

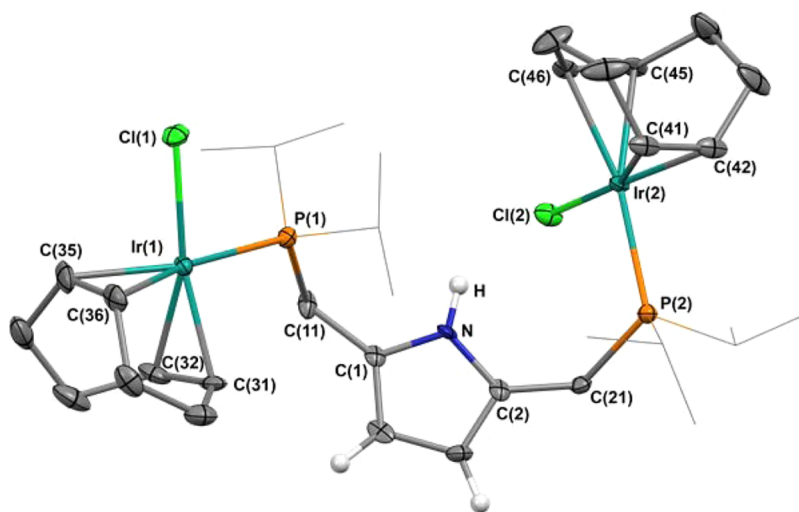


Figure 1. Thermal-ellipsoid (50% probability level) representation of [(PN^{PP}P)H{Ir(COD)Cl}₂] (2). Most hydrogen atoms were omitted for clarity. Selected distances (Å) and angles (deg): Ir(1)–Cl(1) = 2.3467(16), Ir(1)–P(1) = 2.3270(16), Ir(1)–C(31) = 2.104(6), Ir(1)–C(32) = 2.125(6), C(31)–C(32) = 1.404(9), Ir(1)–C(35) = 2.179(6), Ir(1)–C(36) = 2.171(6); C(35)–C(36) = 1.390(10), Ir(2)–Cl(2) = 2.3590(16), Ir(2)–P(2) = 2.3311(17), Ir(2)–C(41) = 2.117(6), Ir(2)–C(42) = 2.099(6); C(41)–C(42) = 1.395(9), Ir(2)–C(45) = 2.174(6), Ir(2)–C(46) = 2.196(6), C(45)–C(46) = 1.375(9). P(1)–Ir(1)–Cl(1) = 89.94(6), P(2)–Ir(2)–Cl(2) = 90.65(6).

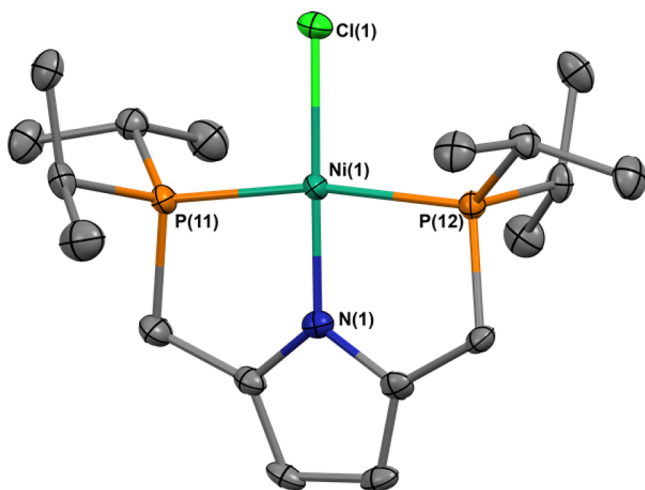
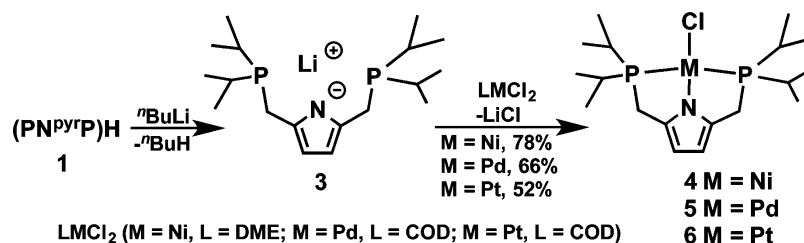
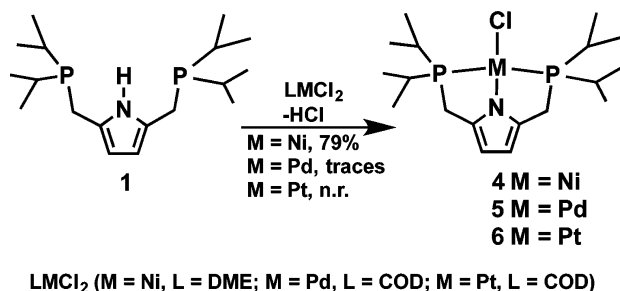
Scheme 1. Synthesis of Metal Complexes from [(PN^{pyr}P)Li]

Figure 2. Thermal-ellipsoid (50% probability level) representation of [(PN^{pyr}P)NiCl] (**4**). Only one of the two crystallographically independent molecules is shown. Hydrogen atoms were omitted for clarity. Selected distances (Å) and angles (deg): Ni(1)–Cl(1) = 2.1688(9), Ni(1)–N(1) = 1.849(2), Ni(1)–P(11) = 2.1963(9), Ni(1)–P(12) = 2.1955(9), P(11)–Ni(1)–Cl(1) = 95.80(3), P(12)–Ni(1)–Cl(1) = 95.45(3), P(11)–Ni(1)–N(1) = 84.48(8), P(12)–Ni(1)–N(1) = 84.19(8), N(1)–Ni(1)–Cl(1) = 178.97(9), P(11)–Ni(1)–P(12) = 167.84(4).

Scheme 2. Synthesis of Metal Complexes from (PN^{pyr}P)H

Despite these positive initial results with group 10 metals, a means to form an iridium PN^{pyr}P complex was still desirable. Tonzetchi^{23,24} and Mani²² reported that triethylamine can be used as a base to form Et₃NH⁺Cl[−] upon the addition of a chlorinated metal reagent such as NiCl₂, [(DME)NiCl₂] or [PdCl₂(PhCN)₂]. Consequently, the reaction between (PN^{pyr}P)H, [Ir(COD)Cl]₂, and NEt₃ in C₆D₆ was carried out. The initial ¹H NMR spectrum was consistent with the immediate formation of the bimetallic species **2** and unreacted free ligand, but, in less than 18 h, a new major product, [(PN^{pyr}P)Ir(COD)] (**7**, ~85% conversion from the starting material) was characterized by a broad singlet at 44.3 ppm in the corresponding ³¹P{¹H} NMR spectrum. Unfortunately, this

reaction could not be scaled up in order to isolate and characterize this product, however, **7** was isolated from another reaction as described below.

Transmetalation with thallium. We became interested in using a thallium transfer reagent because of its milder reducing nature compared to that of Li or Na analogues.^{41–43} Precedent has been reported for the successful transmetalation of thallium-tridentate ligands containing a central anionic nitrogen donor to group 10 metals.^{41,42} Consequently, the feasibility of thallium transmetalation was assessed with PN^{pyr}P, first to group 10 and then to other transition metals.

Compound [(PN^{pyr}P)Tl] (**8**) was isolated in 96% yield and characterized crystallographically and by ¹H, ¹³C{¹H}, ³¹P{¹H} and ²⁰⁵Tl NMR spectroscopy. The ¹H NMR spectrum is consistent with a tridentate metal complex, similar to the solution structure of [(PNP)Tl] (PNP = bis(2-di-*iso*-propylphosphino)-4-methylphenyl)amide.⁴¹ The ¹³C{¹H} NMR spectrum further shows virtual triplets for the resonances corresponding to the methylene and *iso*-propyl groups on the pyrrole side arms indicating the bound nature of the phosphine donors. However, a sharp singlet was observed in the ³¹P{¹H} NMR spectrum (C₆D₆) at 39.31 ppm, contrary to an expected doublet (or two doublets), as observed in other cases,^{41,44} as a result of phosphorus coupling to thallium's active isotopes (²⁰³Tl, *I* = 1/2, 29.5%; ²⁰⁵Tl, *I* = 1/2, 70.5%). Variable temperature NMR spectroscopy studies were undertaken in order to resolve the expected underlying Tl–P coupling. However, lowering the temperature to –80 °C in toluene-*d*₈ led, below –40 °C, to the disappearance into the baseline of all resonances present in the ¹H and ³¹P{¹H} NMR spectra. The ²⁰⁵Tl NMR spectrum also features a singlet at 3139.99 ppm, and no coupling with ³¹P was observed. We hypothesize that a fast exchange occurs in **8** through an oligomeric species that does not allow the observation of Tl–P coupling at room temperature. At lower temperatures, this exchange is slower and all resonances become broad and indistinguishable.

Interestingly, the solid state molecular structure of **8** (Figure 3) indicates that the two phosphorus atoms are at a distance of 3.407 and 3.476 Å from thallium. These distances are considerably longer than those observed for other tricoordinated thallium complexes, including the [(PNP)Tl] analog (Tl–P = 2.971 Å, 3.108 Å)⁴¹ and three complexes containing tripodal phosphine donor ligands ([PhB(CH₂P^{Pr}₂)₃]₃Tl,⁴⁵ [PhB(CH₂PPh₂)₃]₃Tl,⁴⁴ [PhBP₃^{CF₃Ph}]₃Tl,⁴⁶ (Tl–P = 2.894–2.965 Å). The Tl–P distance in **8** is longer than would be reasonable for a strong bonding interactions in the solid state (sum of covalent radii of Tl and P is 2.52 Å, sum of van der Waals radii is 3.76 Å),^{47,48} but a stronger interaction is present in solution based on the spectroscopic data. Upon expansion of the unit cell (Figure 3), an η²-type intermolecular interaction with the pyrrole backbone of another [(PN^{pyr}P)Tl] molecule is observed; the Tl–C(3)# (2.897(3) Å) and Tl–C(4)# distances

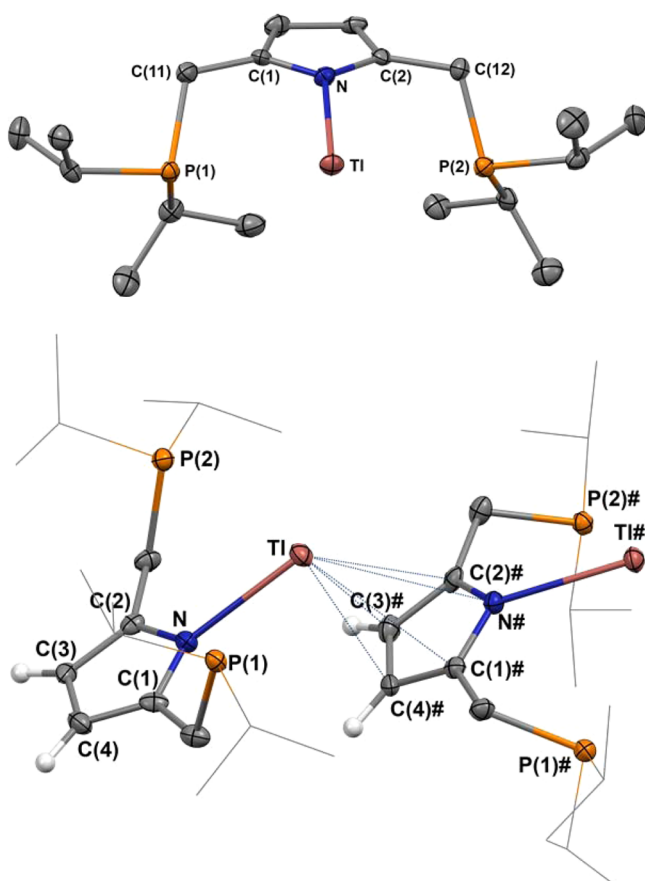


Figure 3. Thermal-ellipsoid (50% probability level) representation of $[(\text{PN}^{\text{pyr}}\text{P})\text{Tl}]$ (**8**). Most hydrogen atoms were omitted for clarity. Selected distances (\AA) and angles (deg): $\text{Tl}-\text{N} = 2.532(2)$, $\text{Tl}-\text{C}(3)\# = 2.897(3)$, $\text{Tl}-\text{C}(4)\# = 2.932(4)$, $\text{Tl}-\text{C}(1)\# = 3.260(3)$, $\text{Tl}-\text{C}(2)\# = 3.225(3)$, $\text{Tl}-\text{N}\# = 3.448(2)$, $\text{C}(3)-\text{C}(4) = 1.406(5)$, $\text{Tl}-\text{P}(1) = 3.4068(8)$, $\text{Tl}-\text{P}(2) = 3.4762(9)$.

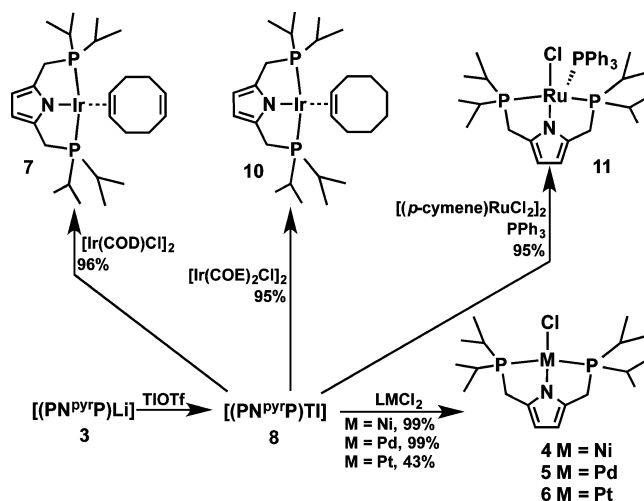
($2.932(4) \text{\AA}$) are considerably shorter than the $\text{Tl}-\text{C}(1)\#$ and $\text{Tl}-\text{C}(2)\#$ distances ($3.260(3)$ and $3.225(3) \text{\AA}$, respectively) demonstrating that the thallium atom sits directly above the $\text{C}(3)\#-\text{C}(4)\#$ bond instead of above the entire pyrrole ring. The overall observed structure is less common than other reported polymeric structures because it does not consist of chains of $\text{Tl}-\text{Tl}$ interactions or take advantage of alternating $\text{Tl}-\eta^5/\eta^6$ interactions, as appears to be common. Only one other structure could be found exhibiting an alternating $\text{Tl}-\eta^2$ polymeric chain structure; the thallium atom from $[(m,m-(\text{CH}_3)_2\text{Ph})_2\text{B}(\text{CH}_2\text{P}^t\text{Bu}_2)_2]\text{Tl}$ coordinates to the two phosphine donors ($\text{Tl}-\text{P} = 2.992$ and 2.942\AA) and displays a weak η^2 -type interaction with the substituted phenyl ring of a neighboring molecule ($\text{Tl}-\text{C} = 3.353$ and 3.388\AA).⁴⁹

DFT calculations were employed to understand the electronic structure of $[(\text{PN}^{\text{pyr}}\text{P})\text{Tl}]$ further. The structural parameters of the optimized geometry for a monomeric $[(\text{PN}^{\text{pyr}}\text{P})\text{Tl}]$ (Table S2 and Figure S1) resemble those of the structure determined by X-ray diffraction and no phosphine coordination to the metal center is observed. A localized energetic minimum with the phosphine arms coordinated to the metal center could not be found. We also optimized a series of oligomers $[(\text{PN}^{\text{pyr}}\text{P})\text{Tl}]_x$ ($[\mathbf{8}]_x$, $x = 2-6$) in order to calculate the stabilization for the interaction between the thallium center and the pyrrole ring of a neighboring molecule.

The energy gain was consistent for the different oligomers studied, with values of $6.0-6.3 \text{ kcal/mol}$.

From this newly characterized $[(\text{PN}^{\text{pyr}}\text{P})\text{Tl}]$ species, transmetalations with group 10 metal chlorides were carried out (Scheme 3). These reactions were performed in tetrahydrofur-

Scheme 3. Synthesis of $[(\text{PN}^{\text{pyr}}\text{P})\text{Tl}]$ (**8**) and Its Transmetalation Reactions



an, allowing quick precipitation of TlCl and nearly quantitative yields of $[(\text{PN}^{\text{pyr}}\text{P})\text{MCl}]$ ($\text{M} = \text{Ni}$, **4**; Pd , **5**) and 43% of $[(\text{PN}^{\text{pyr}}\text{P})\text{PtCl}]$, (**6**) upon filtration. Compound **6** was recrystallized from a concentrated dichloromethane solution layered with Et_2O and was characterized by X-ray diffraction (Figure 4). NMR spectroscopy indicates that the solution structures of all three complexes are similar.

Transmetalation of thallium PNP species to form iridium and ruthenium complexes has not been described. Thus, the

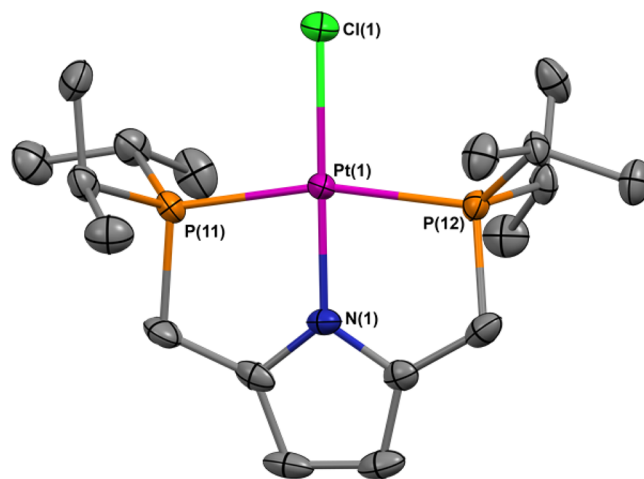


Figure 4. Thermal-ellipsoid (50% probability level) representation of $[(\text{PN}^{\text{pyr}}\text{P})\text{PtCl}]$ (**6**). Only one of the two crystallographically independent molecules is shown. Hydrogen atoms were omitted for clarity. Selected distances (\AA) and angles (deg): $\text{Pt}(1)-\text{Cl}(1) = 2.3135(14)$, $\text{Pt}(1)-\text{N}(1) = 1.966(4)$, $\text{Pt}(1)-\text{P}(11) = 2.2789(14)$, $\text{Pt}(1)-\text{P}(12) = 2.2802(14)$, $\text{P}(11)-\text{Pt}(1)-\text{Cl}(1) = 97.97(5)$, $\text{P}(12)-\text{Pt}(1)-\text{Cl}(1) = 96.98(5)$, $\text{P}(11)-\text{Pt}(1)-\text{N}(1) = 82.47(13)$, $\text{P}(12)-\text{Pt}(1)-\text{N}(1) = 82.57(13)$, $\text{N}(1)-\text{Pt}(1)-\text{Cl}(1) = 179.46(13)$, $\text{P}(11)-\text{Pt}(1)-\text{P}(12) = 164.30(5)$.

reaction of $[(\text{PN}^{\text{pyr}}\text{P})\text{TI}]$ (**8**) with half an equivalent of $[\text{Ir}(\text{COD})\text{Cl}]_2$ was carried out and led, notably, to the product that was previously observed in the deprotonation attempt with NEt_3 , $[(\text{PN}^{\text{pyr}}\text{P})\text{Ir}(\text{COD})]$ (**7**). ^1H NMR spectroscopy indicates that COD is monocoordinated to the metal center. Resonances are observed at 6.53, 5.86, and 3.40 ppm (in C_6D_6), integrating to two protons each which represent the pyrrole backbone, unbound COD, and bound COD olefinic protons, respectively. The differentiation between the bound and unbound COD olefin protons was made assuming that the iridium metal center engages in π -back bonding with the bound olefin, reducing its bond order and shifting its protons upfield compared to the unbound olefin protons. This conclusion is supported by $^{13}\text{C}\{^1\text{H}\}$ and HSQC NMR spectroscopy: the unbound and bound olefinic carbons are observed nearly 80 ppm apart, at 131.10 and 45.32 ppm, respectively. Interestingly, upon crystallization, a different compound is obtained, $[(\text{PN}^{\text{pyr}}\text{P})\text{Ir}]_2(\text{COD})$ (**9**), in which the COD ligand bridges the two iridium metal centers (Figure 5).

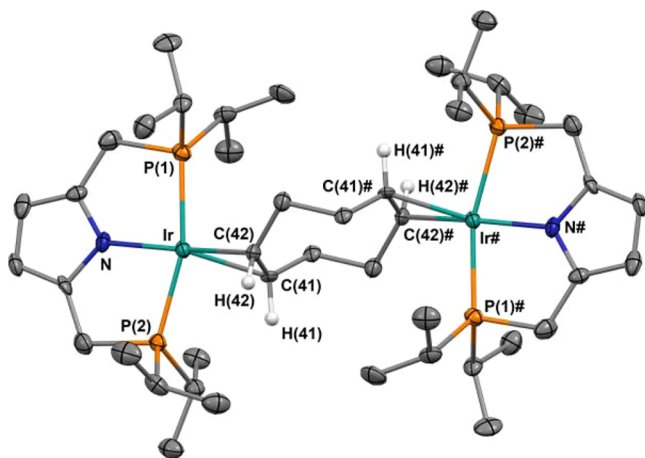


Figure 5. Thermal-ellipsoid (50% probability level) representation of $[(\text{PN}^{\text{pyr}}\text{P})\text{Ir}]_2(\text{COD})$ (**9**). Most hydrogen atoms were omitted for clarity. Selected distances (Å) and angles (deg): Ir–P(1) = 2.3344(16), Ir–P(2) = 2.2929(16), Ir–N = 2.023(4), Ir–C(41) = 2.152(6), Ir–C(42) = 2.147(5), C(41)–C(42) = 1.428(8), P(1)–Ir–P(2) = 162.26(6), P(1)–Ir–N = 81.32(14), P(2)–Ir–N = 81.180(14).

A search through the Cambridge Structural Database showed two examples in which a COD ligand bridges two iridium centers through both double bonds, though neither of these complexes exhibits a square planar geometry at iridium.^{50,51} Compared to other neutral, square planar iridium PNP complexes containing an anionic nitrogen donor and COE, $[(\text{PN}^{\text{pyr}}\text{P})\text{Ir}]_2(\text{COD})$ has similar metrical parameters.^{52–54} These parameters are also similar to other neutral iridium PNP systems containing olefins.^{55–57}

Consistent with the isolation of $[(\text{PN}^{\text{pyr}}\text{P})\text{Ir}(\text{COD})]$ (**7**), the reaction between $[\text{Ir}(\text{COE})_2\text{Cl}]_2$ and $[(\text{PN}^{\text{pyr}}\text{P})\text{TI}]$ led to the formation of $[(\text{PN}^{\text{pyr}}\text{P})\text{Ir}(\text{COE})]$ (**10**). The ^1H NMR spectrum of **10** shows resonances at 6.52 and 3.14 ppm, representing the pyrrole backbone and bound COE olefin protons, respectively.

Given the success of thallium transmetalation reactions to iridium, the synthesis of a ruthenium complex was also pursued. Similar to iridium, attempts involving the protonated ligand or a lithium pyrrolide species led to intractable mixtures of products. Reactions between $[(\text{PN}^{\text{pyr}}\text{P})\text{TI}]$ and $[(p\text{-cymene})\text{-}$

RuCl_2]₂ were run in the presence of a phosphine ligand (PPh_3) in order to promote the formation of a stable 16-electron Ru(II) complex. Therefore, $[(p\text{-cymene})\text{Ru}(\text{PPh}_3)\text{Cl}_2]$ ⁵⁸ was generated *in situ* before the addition of $[(\text{PN}^{\text{pyr}}\text{P})\text{TI}]$. Compound $[(\text{PN}^{\text{pyr}}\text{P})\text{Ru}(\text{PPh}_3)\text{Cl}]$ (**11**, Scheme 3) was isolated as a forest green solid by extraction in C_6H_6 and recrystallization from a concentrated toluene solution layered with *n*-pentane. Dichroic single crystals (forest green/rusty orange) were grown from a concentrated toluene solution (Figure 6). A distorted square pyramidal structure is observed

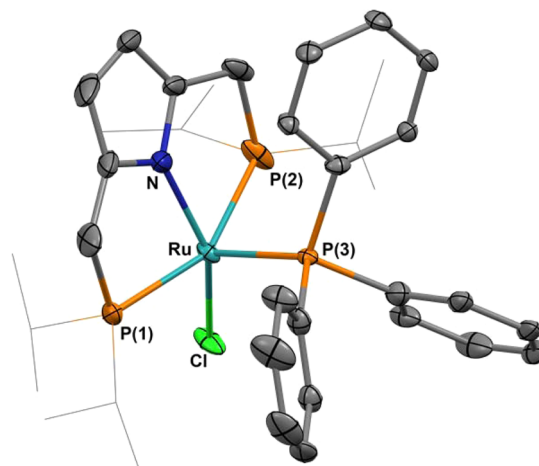


Figure 6. Thermal-ellipsoid (50% probability level) representation of $[(\text{PN}^{\text{pyr}}\text{P})\text{Ru}(\text{PPh}_3)\text{Cl}]$ (**11**). Hydrogen atoms were omitted for clarity. Selected distances (Å) and angles (deg): Ru–P(1) = 2.3767(11); Ru–P(2) = 2.3410(12); Ru–P(3) = 2.1953(10); Ru–N = 2.022(3); Ru–Cl = 2.326(3); N–Ru–Cl = 150.97(18); P(1)–Ru–P(2) = 154.26(5); P(1)–Ru–N = 79.43(11); P(2)–Ru–N = 80.42(11); P(1)–Ru–Cl = 95.99(8); P(2)–Ru–Cl = 93.89(10); N–Ru–P(3) = 94.32(10), P(1)–Ru–P(3) = 103.20(4), P(2)–Ru–P(3) = 94.12(4), Cl–Ru–P(3) = 114.55(14).

with the $\text{PN}^{\text{pyr}}\text{P}$ and Cl ligands in one plane, and PPh_3 in the apical position. Complex **11** displays similar metrical parameters to other neutral, square pyramidal Ru(II) compounds containing tridentate ligands,^{59–65} and is also structurally similar to the cationic five-coordinate Ru(II) complex $[\text{RuCl}(\text{PPh}_3)(\text{PNN})]\text{OTf}$ (PNN = 2-di-*tert*-butylphosphinomethyl-6-diethylaminomethylpyridine).⁶⁶

Since the removal of excess PPh_3 proved difficult at times, analogous reactions with PMe_3 , a volatile phosphine, were carried out. Unfortunately, attempts to isolate $[(p\text{-cymene})\text{Ru}(\text{PMe}_3)\text{Cl}_2]$ or to generate it *in situ* were not successful.⁵⁸

Transmetalation with silver. Silver complexes with both anionic⁴¹ and neutral⁶⁷ PNP ligands have been previously investigated as transmetalation reagents. In order to assess its utility, compound $[(\text{PN}^{\text{pyr}}\text{P})\text{Ag}]_2$ (**12**) was synthesized by two methods, starting with Ag_2O or AgPF_6 (Scheme 4), similarly to what was reported by Mendiola and Ozerov.⁴¹ Both methods afforded a clean product, with the second method leading to higher yields than the first. ^1H NMR spectroscopy indicates a time-averaged symmetric solution structure, and the corresponding $^{31}\text{P}\{^1\text{H}\}$ NMR spectrum shows two nearly overlapping doublets (19.93 ppm, $J_{\text{Ag-P}}^{107} = 394$ Hz, $J_{\text{Ag-P}}^{109} = 454$ Hz) due to similar coupling constants from silver's equally abundant active isotopes (^{107}Ag , $I = 1/2$, 51.8%; ^{109}Ag , $I = 1/2$, 48.2%). X-ray crystallography indicates that the solid state molecular structure of **12** is dimeric (Figure 7).

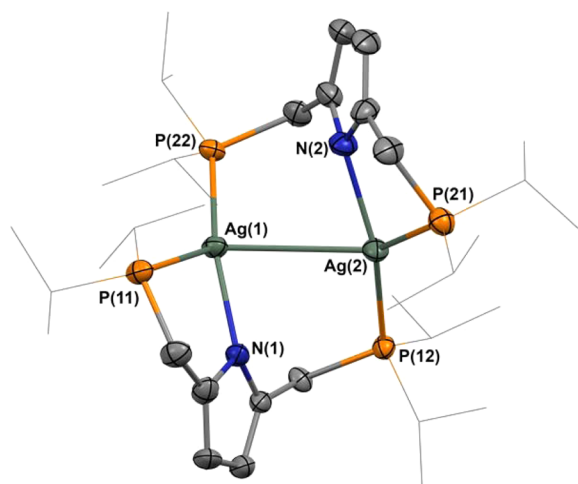
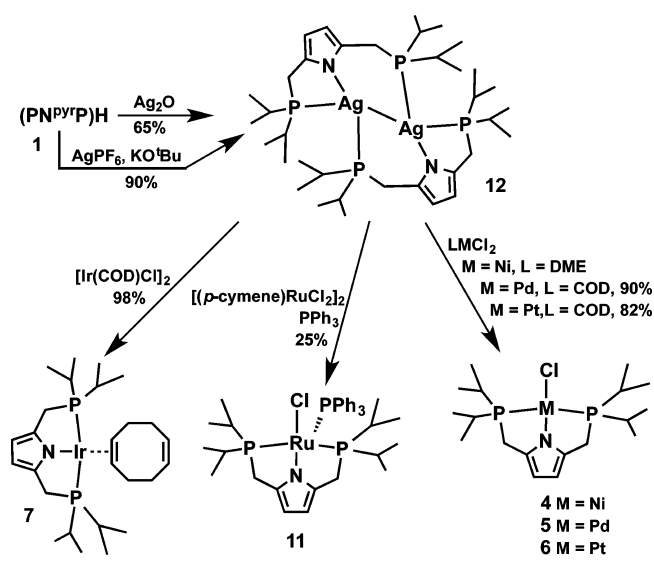
Scheme 4. Synthesis of $[(\text{PN}^{\text{pyr}}\text{P})\text{Ag}]_2$ (**12**) and Its Transmetalation Reactions

Figure 7. Thermal-ellipsoid (50% probability level) representation of $[(\text{PN}^{\text{pyr}}\text{P})\text{Ag}]_2$ (**12**). Hydrogen atoms were omitted for clarity. Selected distances (Å) and angles (deg): Ag(1)–Ag(2) = 3.1730(5), Ag(1)–P(11) = 2.5893(13), Ag(1)–P(22) = 2.3660(12), Ag(1)–N(1) = 2.193(3), Ag(2)–P(21) = 2.5895(13), Ag(2)–P(12) = 2.3791(12), Ag(2)–N(2) = 2.212(4), P(11)–Ag(1)–P(22) = 127.56(4), P(11)–Ag(1)–Ag(2) = 121.69(3), P(11)–Ag(1)–N(1) = 79.23(10), P(22)–Ag(1)–N(1) = 150.96(11), P(22)–Ag(1)–Ag(2) = 94.05(3), N(1)–Ag(1)–Ag(2) = 76.82(9), P(21)–Ag(2)–P(12) = 129.25(4), P(21)–Ag(2)–Ag(1) = 122.97(3), P(21)–Ag(2)–N(2) = 78.42(11), P(12)–Ag(2)–Ag(1) = 92.96(3), P(12)–Ag(2)–N(2) = 151.41(11), N(2)–Ag(2)–Ag(1) = 72.85(10).

Mindiola and Ozerov⁴¹ reported that $[(\text{PNP})\text{Ag}]_2$ is dimeric both in solution and solid state. Since $[(\text{PN}^{\text{pyr}}\text{P})\text{Ag}]_2$ should not be symmetrical in solution and the room temperature ^1H and $^{31}\text{P}\{^1\text{H}\}$ NMR spectra are consistent with a symmetrical species, it is likely that a fluxional process occurs in solution where the central nitrogen donor migrates from one silver atom to another while the complex maintains its dimeric form. The slight broadening observed in both spectra can be explained by invoking an equilibrium between isomers. The $^{13}\text{C}\{^1\text{H}\}$ NMR spectrum of $[(\text{PN}^{\text{pyr}}\text{P})\text{Ag}]_2$ is also less resolved than those of the other complexes described here. Variable temperature ^1H and $^{31}\text{P}\{^1\text{H}\}$ NMR spectra (Figure S58 and S59) are consistent

with the presence of the dimeric structure in solution between -60 and 105 °C. At higher temperature, the broadening of spectra is observed due to a secondary rearrangement process, where the phosphine arms also migrate from one metal to another.

Like the thallium analogue, **12** was first used in transmetalation reactions with group 10 metals. Overall, reactions with $[(\text{PN}^{\text{pyr}}\text{P})\text{Ag}]_2$ proceeded less readily than with $[(\text{PN}^{\text{pyr}}\text{P})\text{Tl}]$. For example, in the reaction to form the nickel product (**4**), a paramagnetic species was obtained in addition to $[(\text{PN}^{\text{pyr}}\text{P})\text{NiCl}]$, as evidenced by the presence of broad resonances in the ^1H NMR spectra of crude reaction mixtures. Also, heating at 65 °C was required in order to observe good conversion to $[(\text{PN}^{\text{pyr}}\text{P})\text{PdCl}]$ or $[(\text{PN}^{\text{pyr}}\text{P})\text{PtCl}]$.

Compound $[(\text{PN}^{\text{pyr}}\text{P})\text{Ag}]_2$ performed similarly to the thallium agent with respect to the formation of $[(\text{PN}^{\text{pyr}}\text{P})\text{Ir}(\text{COD})]$. However, the synthesis of $[(\text{PN}^{\text{pyr}}\text{P})\text{Ru}(\text{PPh}_3)\text{Cl}]$ led to results similar to those achieved when using $[(\text{PN}^{\text{pyr}}\text{P})\text{Li}]$. The formation of $[(p\text{-cymene})\text{Ru}(\text{PPh}_3)\text{Cl}]_2$ from $[(p\text{-cymene})\text{RuCl}_2]_2$ and PPh_3 was first observed, but upon the addition of $[(\text{PN}^{\text{pyr}}\text{P})\text{Ag}]_2$, less than 25% of the desired product was formed together with some unidentified side products. Thus, the use of $[(\text{PN}^{\text{pyr}}\text{P})\text{Tl}]$ as a transfer agent is crucial for the formation of the ruthenium product, although $[(\text{PN}^{\text{pyr}}\text{P})\text{Tl}]$ and $[(\text{PN}^{\text{pyr}}\text{P})\text{Ag}]_2$ were equally efficient for the synthesis of $[(\text{PN}^{\text{pyr}}\text{P})\text{Ir}(\text{COD})]$.

CONCLUSIONS

A PNP ligand, $\text{PN}^{\text{pyr}}\text{P}$, was designed that employs a pyrrole unit as a central anionic nitrogen donor. In order to expand the knowledge on this class of ligands, an analogue containing di-*iso*-propylphosphine arms was synthesized. The corresponding group 10 metal chlorides as well as iridium and ruthenium complexes were isolated and characterized. The group 10 metal chlorides could be obtained in good yields from multiple synthetic methods and are structurally similar to the other 16-electron, square planar complexes reported with pyrrole-based PNP ligands. However, because the desired iridium and ruthenium complexes could not be isolated using protocols similar to those employed for group 10 metals, $[(\text{PN}^{\text{pyr}}\text{P})\text{Tl}]$ and $[(\text{PN}^{\text{pyr}}\text{P})\text{Ag}]_2$ were synthesized and characterized. The thallium and silver species were paramount in the formation of new iridium and ruthenium complexes, proving their utility as transfer agents. A comparison of these synthetic methods organized for each metal atom is presented in Table 1. Both $[(\text{PN}^{\text{pyr}}\text{P})\text{Ir}]_2(\text{COD})$ and $[(\text{PN}^{\text{pyr}}\text{P})\text{Ru}(\text{PPh}_3)\text{Cl}]$ contain features such as the presence of a labile ligand and an open coordination site that are common to other PNP complexes found to be effective catalysts for dehydrogenation⁶⁶ and their reactivity will be probed in future work.

EXPERIMENTAL SECTION

General considerations. Unless noted otherwise, all experiments were performed under a nitrogen atmosphere in a glovebox. Molecular sieves (4 Å, 1–2 mm beads) were ordered from Alfa Aesar and were activated by heating at 250 °C for 2 days under vacuum on a Schlenk line and then brought into an N_2 -filled glovebox. Hexanes, *n*-pentane, toluene, diethyl ether, tetrahydrofuran, and toluene were stored over molecular sieves in a N_2 -filled glovebox. NET_3 was distilled before being stored in the glovebox. Deuterated solvents were purchased from Cambridge Isotope Laboratories. C_6D_6 was brought in the glovebox, stirred and dried over CaH_2 for 24 h, filtered, and stored over molecular sieves. CDCl_3 was purged with N_2 before being brought into the glovebox and was stored over molecular sieves.

Table 1. Comparison of Synthetic Methods for Discussed Metal Complexes^a

Reagent used	[(PN ^{pyr} P) NiCl] (4)	[(PN ^{pyr} P) PdCl] (5)	[(PN ^{pyr} P) PtCl] (6)	[(PN ^{pyr} P) Ir(COD)] (7)	[(PN ^{pyr} P) Ru(PPh ₃) Cl] (11)
(PN ^{pyr} P)H (1)	78.6%	trace	0%	0%	0%
[(PN ^{pyr} P) Li] (3)	77.9%	66.3%	52.4% ^b	85% ^{b,c}	26.0% ^b
[(PN ^{pyr} P) Tl] (8)	98.8%	>99%	42.9%	95.5%	94.5%
[(PN ^{pyr} P) Ag] ₂ (12)	N/A ^d	90.1%	82.1%	97.5%	25.0% ^b

^aIsolated yields unless otherwise indicated. ^bConversion determined by ³¹P{¹H} NMR spectroscopy. ^cWhen reaction is run in the presence of NEt₃. ^dBroad paramagnetic resonances observed by ¹H NMR spectroscopy.

Triphenylphosphine, silver(I) oxide, and silver hexafluorophosphate were ordered from Alfa Aesar and used as received. [(DME)NiCl₂], [(COD)PdCl₂], [(COD)PtCl₂], [Ir(COD)Cl]₂, [Ir(COE)₂Cl]₂, [(p-cymene)RuCl₂]₂, and TlOTf were ordered from Strem Chemicals and used as received. 2,5-bis(dimethylaminomethyl)pyrrole was synthesized according to a published procedure.⁶⁸ A 1.6 M *n*-BuLi solution in hexanes (Aldrich), and silica (BDH silica gel 60 Å, ECO/60–200 μm) were used as received. NMR spectra were recorded on either a Bruker 400 MHz or Bruker 500 MHz spectrometer; resonances are reported in ppm. For ¹H and ¹³C{¹H} NMR spectra, the residual solvent resonance was used as an internal reference. For ³¹P{¹H} NMR spectra, an external reference of PPh₃ was prepared and locked to –5.0 ppm in C₆D₆. ⁷Li NMR spectra were referenced to an external standard of 1 M LiCl in D₂O at 0 ppm. Gaussian 03 (revision D.02)⁶⁹ was used for all reported calculations. The B3LYP (DFT) method was used to carry out geometry optimizations on model compounds specified in text using the LANL2DZ basis set. The validity of the true minima was checked by the absence of negative frequencies in the energy Hessian.

Note: Extra precautions were taken when working with thallium and disposing its byproducts due to their toxicity. The moisture, oxygen, and light sensitivity of these materials were not probed explicitly. Precautions were taken to avoid their decomposition, as recommended by previous authors.⁴¹ Compound [(PN^{pyr}P)Tl] was generally used within 2 weeks of its preparation and was stored at –34 °C to maintain its integrity.

Synthesis of (PN^{pyr}P)H (1). In a drybox, 2,5-bis(dimethylaminomethyl)pyrrole (2.35 g, 0.0130 mol, brown oil) was weighed in a 50 mL Schlenk flask. Di-*iso*-propylphosphine (4.42 mL, 0.0298 mol) was measured by syringe and added to the Schlenk flask. The flask was sealed, removed from the box, and the reaction stirred at 145 °C for 48 h. The final product was isolated under an inert atmosphere upon eluting the brown oil through a silica plug with hexanes (crude yield = quantitative, purified yield = 3.47 g, 78.3%, honey-brown oil). For 1: ¹H NMR (400 MHz, C₆D₆): δ 8.11 (br s, 1H, NH), 5.92 (d, 2H, ⁴J_{HH} = 2.4 Hz, pyr-H), 2.58 (s, 4H, CH₂), 1.57 (m, 4H, CH(CH₃)₂), 0.97 (dd, ³J_{HH} = 6.0 Hz, ³J_{HP} = 4.0 Hz, 12H, CH(CH₃)₂), 0.94 (app. d, J = 8.0 Hz, 12H, CH(CH₃)₂). ¹³C{¹H} NMR (126 MHz, C₆D₆): δ 127.67 (d, ²J_{CP} = 8.8 Hz, pyr-C), 107.08 (d, ³J_{CP} = 5.0 Hz, pyr-CH), 23.76 (d, ¹J_{CP} = 15.1 Hz, CH(CH₃)₂), 21.68 (d, ¹J_{CP} = 20.2 Hz, CH₂), 19.89 (d, ²J_{CP} = 15.1 Hz, CH(CH₃)₂), 19.00 (d, ²J_{CP} = 10.1 Hz, CH(CH₃)₂). ³¹P{¹H} NMR (162 MHz, C₆D₆): δ 1.35 (s).

Synthesis of [(PN^{pyr}P)H]Ir(COD)Cl₂ (2). (PN^{pyr}P)H (1, 0.035 g, 0.107 mmol) was dissolved in tetrahydrofuran and the resulting solution stirred at –78 °C for 15 min. [Ir(COD)Cl]₂ (0.0359 g, 0.0534 mmol) was added to the cold tetrahydrofuran solution and the mixture stirred at low temperature for 30 min and at room temperature for 1.5 h. The volatiles were removed under reduced pressure and the resulting orange product was triturated, and extracted sequentially with *n*-pentane, toluene, tetrahydrofuran, and dichloro-

methane. The final, pure bimetallic product was isolated from the dichloromethane extract (yield = 0.012 g, 18.2%), though it was also observed in small amounts in the toluene and tetrahydrofuran extracts. A monometallic species was also observed as the major component of the toluene and tetrahydrofuran extracts and characterized by ³¹P{¹H} NMR shifts at 4.04 ppm (free phosphine) and 18.62 ppm (Ir–P), which are intermediate in value to those of the pure bimetallic complex 2 (20.06 ppm) and pure free ligand (1.35 ppm). Pure free ligand was recovered from the *n*-pentane extract. For 2: ¹H NMR: (400 MHz, C₆D₆): δ 9.98 (br s, 1H, NH), 5.87 (s, 2H, pyr-H), 5.27 (m, 4H, COD-olefin), 3.23 (d, ²J_{HP} = 8.0 Hz, 4H, CH₂), 3.20 (m, 4H, –CH₂–CH=CH–CH₂–), 2.26 (m, 4H, CH(CH₃)₂), 2.11–1.96 (m, 8H, –CH₂–CH=CH–CH₂–), 1.57–1.46 (m, 8H, –CH₂–CH=CH–CH₂–), 1.17 (app. quartet (dvt), 12H, CH(CH₃)₂), 1.08 (app. quartet (dvt), 12H, CH(CH₃)₂). ¹³C{¹H} NMR: (100 MHz, CDCl₃): δ 123.83 (m, pyr-C), 108.40 (s, pyr-CH), 91.33 (d, ³J_{CP} = 14.0 Hz, COD-olefin), 52.01 (s, COD-olefin), 33.98 (s, COD-alkyl), 28.94 (s, COD-alkyl), 24.16 (d, ¹J_{CP} = 26.0 Hz, CH(CH₃)₂), 19.40 (s, CH(CH₃)₂), 18.50 (s, CH(CH₃)₂), 16.47 (d, ¹J_{CP} = 24.0 Hz, –CH₂–). ³¹P{¹H} NMR (162 MHz, C₆D₆): δ 20.06 (s). Anal. Calcd for C₃₄H₅₉Cl₂Ir₂NP₂: C, 40.87; H, 5.95; N 1.40. Found: C, 40.59; H, 6.11; N 1.44.

Synthesis of [(PN^{pyr}P)Li] (3). In a 20 mL scintillation vial, (PN^{pyr}P)H (0.1416 g, 0.433 mmol) was dissolved in hexanes and chilled at –78 °C for 30 min. ⁿBuLi (1.6 M, 0.265 mL, 0.424 mmol) was added dropwise and the solution was stirred cold for 30 min and at room temperature for 1.5 h. A white precipitate ([(PN^{pyr}P)Li]) was observed at low temperature but appeared to be soluble in hexanes at room temperature and could not be isolated by filtration. The volatiles were removed under reduced pressure and the pale-yellow oily solution was set to recrystallize at –35 °C. A small amount of an off-white solid was recrystallized from the oily red mixture of products (yield = 0.0247 g, 17.1%). For 3: ¹H NMR: (400 MHz, C₆D₆): δ 6.24 (s, 2H, pyr-H), 3.21 (s, 4H, –CH₂–), 1.70 (m, 4H, CH(CH₃)₂), 1.08 (app. quartet (dvt), 12H, CH(CH₃)₂), 0.98 (app. quartet (dvt), 12H, CH(CH₃)₂). ¹³C{¹H} NMR (126 MHz, C₆D₆): δ 135.86 (s, pyr-C), 108.59 (s, pyr-CH), 25.65 (s, CH(CH₃)₂), 22.57 (s, –CH₂–), 19.79 (s, CH(CH₃)₂), 19.37 (s, CH(CH₃)₂). ³¹P{¹H} NMR (162 MHz, C₆D₆): δ –1.01 (septet, ¹J_{PLi} = 25 Hz). ⁷Li NMR (194 MHz, C₆D₆): 2.50 (pentet, ¹J_{LIP} = 25 Hz).

Synthesis of [(PN^{pyr}P)NiCl] (4). *Method A, from (PN^{pyr}P)H (1).* In a 20 mL scintillation vial, (PN^{pyr}P)H (0.0262 g, 0.0800 mmol) was weighed, dissolved in tetrahydrofuran, and chilled at –34 °C for 30 min. [(DME)NiCl₂] (0.0176 g, 0.0800 mmol) was separately weighed and added to the stirring (PN^{pyr}P)H solution by spatula and then as a slurry in tetrahydrofuran. The reaction quickly changed from pale yellow to a deep orange/red solution. After 5 min, a blue/green precipitate was observed to be stuck to the bottom and sides of the vial. After 1.5 h, the clear orange tetrahydrofuran solution was filtered into a new vial, and the volatiles were removed under reduced pressure. ¹H NMR spectroscopy indicates that the tetrahydrofuran soluble extract (0.0265 g, 78.6%) was clean [(PN^{pyr}P)NiCl] (4), while the precipitate had broad resonances in the ¹H NMR spectrum. Further identification of this byproduct was not attempted.

Method B, from [(PN^{pyr}P)Li] (2). In a 20 mL standard scintillation vial, a stirring tetrahydrofuran solution of (PN^{pyr}P)H (1, 0.050 g, 0.153 mmol) was cooled to –78 °C. By syringe, ⁿBuLi (1.6 M, 0.105 mL, 0.168 mmol) was measured and added slowly to the cold solution, and stirred for 30 min at low temperature. [(DME)NiCl₂] (0.0436 g, 0.199 mmol) was weighed and added to the reaction at low temperature. The reaction vial was then removed from the cold well and the solution stirred at room temperature. After 2 h, the volatiles were removed under reduced pressure, *n*-pentane was added to the reaction vial, the solution filtered, and the volatiles removed in order to give a deep orange/red powder (yield = 0.050 g, 77.9%).

Method C, from [(PN^{pyr}P)Tl] (8). To a stirring tetrahydrofuran solution of [(PN^{pyr}P)Tl] (8) (0.0672 g, 0.127 mmol), a tetrahydrofuran solution of [(DME)NiCl₂] (0.0306 g, 0.139 mmol) was added dropwise. The clear, light brown solution became cloudy quickly and lighter in color before becoming a deeper orange. After 30 min, the reaction was filtered to give a white precipitate (TlCl) and a

bright orange solution of $[(\text{PN}^{\text{pyr}}\text{P})\text{NiCl}]$. No further purification was necessary (yield: 0.0526 g, 98.9%).

Method D, from $[(\text{PN}^{\text{pyr}}\text{P})\text{Ag}]_2$ (12). $[(\text{PN}^{\text{pyr}}\text{P})\text{Ag}]_2$ (3, 0.0841 g, 0.0968 mmol) was weighed in a vial wrapped in foil containing a stir bar, and dissolved in Et_2O . $[(\text{DME})\text{NiCl}_2]$ (0.0425 g, 0.194 mmol) was weighed in a separate vial and added to the solution of 3, first as a solid and then as a slurry in Et_2O . The solution quickly became brighter in color: after 15 min was filtered to give a clear orange solution, becoming a fine orange powder upon removal of Et_2O . Although $^{31}\text{P}\{^1\text{H}\}$ NMR spectroscopy indicated a quantitative conversion to $[(\text{PN}^{\text{pyr}}\text{P})\text{NiCl}]$, ^1H NMR spectroscopy revealed the presence of multiple, large broad resonances, indicating that a paramagnetic species may be present in addition to the expected diamagnetic product. For 4: ^1H NMR: (400 MHz, C_6D_6): δ 6.30 (s, 2H, pyr-H), 2.49 (app. t, $J_{\text{HP}} = 4.0$ Hz, 4H, $-\text{CH}_2-$), 1.91 (m, 4H, $\text{CH}(\text{CH}_3)_2$), 1.40 (app. quartet (dvt), 12H, $\text{CH}(\text{CH}_3)_2$), 1.01 (app. quartet (dvt), 12H, $\text{CH}(\text{CH}_3)_2$). $^{13}\text{C}\{^1\text{H}\}$ NMR (100 MHz, C_6D_6): δ 137.93 (s, pyr-C), 105.91 (app. t, $J_{\text{CP}} = 5$ Hz, pyr-CH), 23.59 (app. t, $J_{\text{CP}} = 11.0$ Hz, $\text{CH}(\text{CH}_3)_2$), 22.01 (app. t, $J_{\text{CP}} = 10.0$ Hz, $-\text{CH}_2-$), 18.56 (s, $\text{CH}(\text{CH}_3)_2$), 17.60 (s, $\text{CH}(\text{CH}_3)_2$). $^{31}\text{P}\{^1\text{H}\}$ NMR (162 MHz, C_6D_6): δ 60.53 (s). Anal. Calcd for $\text{C}_{18}\text{H}_{34}\text{ClNiN}_2\text{P}_2$: C, 51.41; H, 8.15; N 3.33. Found: C, 51.05; H, 7.94; N 3.33.

Synthesis of $[(\text{PN}^{\text{pyr}}\text{P})\text{PdCl}]$ (5). **Method A, from $(\text{PN}^{\text{pyr}}\text{P})\text{H}$ (1).** In a 20 mL scintillation vial, $(\text{PN}^{\text{pyr}}\text{P})\text{H}$ (1, 0.0297 g, 0.0907 mmol) was weighed, dissolved in 5 mL of tetrahydrofuran, and chilled at -34°C for 30 min. After chilling, $[(\text{COD})\text{PdCl}_2]$ (0.0259 g, 0.0907 mmol) was separately weighed and added to the stirring $(\text{PN}^{\text{pyr}}\text{P})\text{H}$ solution by spatula and then as a slurry in tetrahydrofuran. The solution color quickly changed from pale yellow to bright yellow as the palladium starting material was solubilized. No additional changes were observed, and after 1.5 h the volatiles were removed. ^1H NMR spectra of crude reaction mixtures taken in CDCl_3 showed broad resonances at 9.7–10 ppm (N-H), 5.78–5.94 (pyr-H), 3.3–3.45 (CH_2), 2.36–2.50 ($\text{CH}(\text{CH}_3)_2$), 1.15–1.3 ($\text{CH}(\text{CH}_3)_2$), while the corresponding $^{31}\text{P}\{^1\text{H}\}$ NMR spectra showed two singlets at 29.9 and 32.0 ppm. This product is likely similar to that observed by Mani, $[\text{Pd}_2\text{Cl}_4\{\mu\text{-C}_6\text{H}_3\text{N-2,5-(CH}_2\text{PPh}_2)_2\text{-}\kappa^2\text{PP}}\}_2]$,²² in which two of the protonated ligands bridge two palladium centers, forming an overall dimeric structure. This is also supported by $^{13}\text{C}\{^1\text{H}\}$ NMR spectroscopy, which shows doublets for the pyrrole unit, indicating P–C coupling to only one proximal phosphorus atom. A small amount (<1%) of the desired product was observed as a singlet at 64.59 ppm by $^{31}\text{P}\{^1\text{H}\}$ NMR spectroscopy (CDCl_3).

Method B, from $[(\text{PN}^{\text{pyr}}\text{P})\text{Li}]$ (2). $(\text{PN}^{\text{pyr}}\text{P})\text{H}$ (1, 0.0774 g, 0.236 mmol) was weighed, dissolved in tetrahydrofuran, and stirred at -78°C for 15 min. $^n\text{BuLi}$ (1.6 M, 0.162 mL, 0.260 mmol) was measured by syringe, diluted with 5 mL tetrahydrofuran, added slowly to the other solution at low temperature, and the resulting mixture stirred for 15 min at low temperature and 1.5 h at room temperature. The solution became darker upon the addition of $[(\text{COD})\text{PdCl}_2]$ (0.0904 g, 0.317 mmol, 5 mL tetrahydrofuran) and then a clear, bright brown when stopped. The volatiles were removed under reduced pressure and toluene was added to promote the precipitation of LiCl. The cloudy brown toluene solution was filtered to give a red-brown precipitate and a brick-red filtrate, affording the product in good yield upon removal of the volatiles (yield = 0.0734 g, 66.3%).

Method C, from $[(\text{PN}^{\text{pyr}}\text{P})\text{Ti}]$ (8). $[(\text{PN}^{\text{pyr}}\text{P})\text{Ti}]$ (8, 0.0426 g, 0.0800 mmol) was weighed in a vial with a stir bar and dissolved in toluene. $[(\text{COD})\text{PdCl}_2]$ (0.0266 g, 0.0931 mmol) was weighed separately in a vial, dissolved in toluene, and added slowly to the $[(\text{PN}^{\text{pyr}}\text{P})\text{Ti}]$ solution. The solution gradually became orange in color with an obvious white precipitate. After 2 h, the reaction was filtered into a clean vial, the volatiles removed under reduced pressure to yield a bright orange solid in quantitative yield.

Method D, from $[(\text{PN}^{\text{pyr}}\text{P})\text{Ag}]_2$ (12). $[(\text{PN}^{\text{pyr}}\text{P})\text{Ag}]_2$ (0.0739 g, 0.0851 mmol) was weighed, dissolved in toluene and added to a Schlenk flask covered in aluminum foil. $[(\text{COD})\text{PdCl}_2]$ (0.0566 g, 0.198 mmol) was also added to the Schlenk flask as a toluene slurry. The flask was heated for 2 h at 65°C and then the toluene solution was filtered under an inert atmosphere. Toluene was removed under

reduced pressure to give a red-orange product (yield = 0.0718 g, 90.1%). For 7: ^1H NMR: (500 MHz, C_6D_6): δ 6.38 (s, 2H, pyr-H), 2.70 (app. t, $J_{\text{HP}} = 5$ Hz, 4H, $-\text{CH}_2-$), 1.92 (m, 4H, $\text{CH}(\text{CH}_3)_2$), 1.28 (app. quartet (dvt), 12H, $\text{CH}(\text{CH}_3)_2$), 0.90 (app. quartet (dvt), 12H, $\text{CH}(\text{CH}_3)_2$). $^{13}\text{C}\{^1\text{H}\}$ NMR (126 MHz, C_6D_6): δ 137.01 (app. t, $J_{\text{CP}} = 5.0$ Hz, pyr-C), 104.64 (app. t, $J_{\text{CP}} = 6.3$ Hz, pyr-CH), 24.47 (app. t, $J_{\text{CP}} = 11.3$ Hz, $\text{CH}(\text{CH}_3)_2$), 18.56 (app. t, $J_{\text{CP}} = 2.5$ Hz, $-\text{CH}_2-$), 17.66 (s, $\text{CH}(\text{CH}_3)_2$). $^{31}\text{P}\{^1\text{H}\}$ NMR (200 MHz, C_6D_6): δ 63.85 (s). Anal. Calcd for $\text{C}_{18}\text{H}_{34}\text{ClNP}_2\text{Pd}$: C, 47.17; H, 7.32; N 2.99. Found: 45.82; H, 7.26; N 2.86.

Synthesis of $[(\text{PN}^{\text{pyr}}\text{P})\text{PtCl}]$ (6). **Method A, from $(\text{PN}^{\text{pyr}}\text{P})\text{H}$ (1).** In a 20 mL standard scintillation vial, $(\text{PN}^{\text{pyr}}\text{P})\text{H}$ (1, 0.0475 g, 0.145 mmol) was weighed, dissolved in tetrahydrofuran, and chilled at -34°C for 30 min. After chilling, $[(\text{COD})\text{PtCl}_2]$ (0.0543 g, 0.145 mmol) was separately weighed and added to the stirring $(\text{PN}^{\text{pyr}}\text{P})\text{H}$ solution by spatula and then as a slurry in tetrahydrofuran. The solution remained largely unchanged after the addition of $[(\text{COD})\text{PtCl}_2]$, appearing as a pale yellow solution. No additional changes were observed and after 1.5 h the volatiles were removed under reduced pressure. ^1H and $^{31}\text{P}\{^1\text{H}\}$ NMR spectroscopy indicated that unreacted ligand was still present (~40% of products by integration) along with multiple additional side products.

Method B, from $[(\text{PN}^{\text{pyr}}\text{P})\text{Li}]$ (2). $(\text{PN}^{\text{pyr}}\text{P})\text{H}$ (1, 0.0842 g, 0.257 mmol) was weighed, dissolved in tetrahydrofuran, and stirred at -78°C for 15 min. $^n\text{BuLi}$ (1.6 M, 0.177 mL, 0.283 mmol) was measured by syringe, diluted with 5 mL tetrahydrofuran, added slowly to the ligand solution at low temperature, and was stirred for 15 min at low temperature and 1.5 h at room temperature. The solution became darker upon the addition of $[(\text{COD})\text{PtCl}_2]$ (0.116 g, 0.309 mmol) and was a cloudy bright orange-brown solution when stopped. The solution was filtered to give an orange filtrate and an orange-brown precipitate. Upon removal of the volatiles, the product was obtained in 52.4% yield as determined by $^{31}\text{P}\{^1\text{H}\}$ NMR spectroscopy, although 3 additional products were also evident with similar chemical shifts and the desired product was not isolated cleanly.

Method C, from $[(\text{PN}^{\text{pyr}}\text{P})\text{Ti}]$ (8). $[(\text{PN}^{\text{pyr}}\text{P})\text{Ti}]$ (8, 0.0449 g, 0.0846 mmol) was weighed in a vial, dissolved in toluene, and stirred at -78°C for 15 min. $[(\text{COD})\text{PtCl}_2]$ (0.0285 g, 0.0761 mmol) was weighed separately in a vial, dissolved in 5 mL tetrahydrofuran, and added slowly to the $[(\text{PN}^{\text{pyr}}\text{P})\text{Ti}]$ solution at low temperature. The solution turned from pale yellow to pale yellow-orange at low temperature over 10 min. A white precipitate (TiCl) appeared after 5 min at room temperature, at which point the reaction was filtered to give a yellow-orange filtrate and a white precipitate. The product was obtained upon removal of volatiles and was one of two major products observed by $^{31}\text{P}\{^1\text{H}\}$ NMR spectroscopy (60.09 ppm = $[(\text{PN}^{\text{pyr}}\text{P})\text{PtCl}]$, 54.71 = other). The ratio of these two products varied from reaction to reaction, but was often nearly 1:1. Analytically pure, $[(\text{PN}^{\text{pyr}}\text{P})\text{PtCl}]$ (6) was obtained from recrystallization of an tetrahydrofuran solution layered with *n*-pentane (yield = 0.0182 g, 42.9%).

Method D, from $[(\text{PN}^{\text{pyr}}\text{P})\text{Ag}]_2$ (12). $[(\text{PN}^{\text{pyr}}\text{P})\text{Ag}]_2$ (12, 0.0808 g, 0.0930 mmol) was weighed, dissolved in toluene and added to a Schlenk tube covered in aluminum foil. $[(\text{COD})\text{PtCl}_2]$ (0.0785 g, 0.187 mmol) was also added to the Schlenk tube as a toluene slurry. The flask was heated for 4 h at 65°C , then the toluene solution was filtered under an inert atmosphere. Toluene was removed under reduced pressure to give a red-orange product (yield = 0.0853 g, 82.1%). For 6: ^1H NMR: (500 MHz, C_6D_6): δ 6.45 (s, 2H, pyr-H), 2.66 (s, 4H, $-\text{CH}_2-$), 2.06 (m, 4H, $\text{CH}(\text{CH}_3)_2$), 1.28 (app. quartet (dvt), 12H, $\text{CH}(\text{CH}_3)_2$), 0.90 (app. quartet (dvt), 12H, $\text{CH}(\text{CH}_3)_2$). $^{13}\text{C}\{^1\text{H}\}$ NMR (126 MHz, C_6D_6): δ 136.69 (s, pyr-C), 104.22 (app. t, $J_{\text{CP}} = 5.0$ Hz, pyr-CH), 24.41 (app. t, $J_{\text{CP}} = 13.9$ Hz, $-\text{CH}_2-$), 24.38 (app. t, $J_{\text{CP}} = 13.9$ Hz, $\text{CH}(\text{CH}_3)_2$), 18.15 (s, $\text{CH}(\text{CH}_3)_2$), 17.49 (s, $\text{CH}(\text{CH}_3)_2$). $^{31}\text{P}\{^1\text{H}\}$ NMR (200 MHz, C_6D_6): δ 60.09 (s, with Pt satellites, $^1J_{\text{P-Pt}} = 1322$ Hz). Anal. Calcd for $\text{C}_{18}\text{H}_{34}\text{NP}_2\text{Pt-CH}_2\text{Cl}_2$: C, 35.55; H, 5.65; N 2.18. Found: 35.41; H, 5.43; N 2.12.

Synthesis of $[(\text{PN}^{\text{pyr}}\text{P})\text{Ir}(\text{COD})]$ (7). **Method A, from $(\text{PN}^{\text{pyr}}\text{P})\text{H}$ (1).** $(\text{PN}^{\text{pyr}}\text{P})\text{H}$ (1, 0.0251 g, 0.0767 mmol) was weighed, dissolved in C_6D_6 and added to an NMR tube. $[\text{Ir}(\text{COD})\text{Cl}]_2$ (0.0257 g, 0.0353 mmol) was weighed in a vial and added to the NMR tube as a slurry in

C_6D_6 . Finally, 1 drop of NEt_3 was added, the NMR tube was capped, inverted multiple times, and left to sit under an inert atmosphere. The reaction was monitored and after about 18 h, a product formed that remained unchanged up to 4 days. $^{31}P\{^1H\}$ NMR spectroscopy indicated 85% conversion to this product. The formation of $[(PN^{pyr}P)H\{Ir(COD)Cl\}_2]$ (**2**) was also observed.

Method B, from $(PN^{pyr}P)Li$ (2**).** $(PN^{pyr}P)H$ (**1**, 0.0309 g, 0.0944 mmol) was weighed, dissolved in toluene, and stirred at $-78^\circ C$ for 15 min, at which point nBuLi (1.6 M, 0.059 mL, 0.0944 mmol) was added dropwise. The solution was stirred cold for 10 min and at room temperature for 30 min. $[Ir(COD)Cl]_2$ (0.0317 g, 0.0472 mmol) was then weighed separately and added to the $[(PN^{pyr}P)Li]$ solution, turning from bright orange upon initial dissolution of iridium to a brown/rusty orange solution after 45 min when the reaction was stopped. The 1H NMR spectrum contained 4 unresolved hydride resonances, and the regions from 0.0 to 0.4 ppm and 5.5–6.5 ppm were broad with intermittent sharp resonances. The $^{31}P\{^1H\}$ NMR spectrum had a broad baseline from -10 ppm to 10 ppm underneath another broad resonance from 4 to 8 ppm, with other sharp and broad resonances. The product mixture did not appear cleaner after washing and extracting with *n*-pentane. A clean product could not be isolated nor characterized.

Method C, from $[(PN^{pyr}P)TI]$ (8**).** $[(PN^{pyr}P)TI]$ (**8**, 0.0690 g, 0.130 mmol) was dissolved in toluene and left stirring at $-78^\circ C$ for 15 min. $[Ir(COD)Cl]_2$ (0.0437 g, 0.0650 mmol) was weighed separately, dissolved in toluene, and added slowly to the $[(PN^{pyr}P)TI]$ solution at low temperature. The solution was stirred at low temperature for 10 min and room temperature for 15 min, while the solution changed from pale yellow to cloudy orange. The reaction was filtered to give a white precipitate and a bright orange filtrate. Upon drying, a pure bright orange oily product was obtained (yield = 0.0778 g, 95.5%).

Method D, from $[(PN^{pyr}P)Ag]_2$ (12**).** $[(PN^{pyr}P)Ag]_2$ (**12**, 0.0680 g, 0.0783 mmol) was weighed and dissolved in toluene in a vial. $[Ir(COD)Cl]_2$ (0.0528 g, 0.0786 mmol) was weighed separately and added to the vial as a solid and then as a slurry in toluene. The reaction was stirred for 1.5 h at room temperature. The cloudy bright brown solution was filtered to give a deep orange-red filtrate, yielding a deep-red oily solid upon removal of toluene (yield = 0.0965 g, 97.5%). For **7**: 1H (500 MHz, $22^\circ C$, C_6D_6): δ 6.53 (s, 2H, pyr-H), 5.86 (m, 2H, Ir bound $-CH=CH-$), 3.40 (m, 2H, $-CH=CH-$), 2.82 (app. t, $J_{HP} = 5.0$ Hz, 4H, $-CH_2-P^iPr_2$), 2.47 (m, 4H, $-CH_2-CH_2-$), 2.33 (m, 2H, $-CH_2-CH_2-$), 1.86 (m, 4H, $CH(CH_3)_2$), 1.78 (m, 2H, $-CH_2-CH_2-$), 1.10 (app. quartet (dvt), 12H, $CH(CH_3)_2$), 0.90 (app. quartet (dvt), 12H, $CH(CH_3)_2$). $^{13}C\{^1H\}$ NMR: (126 MHz, C_6D_6): δ 140.04 (app. t, $J_{CP} = 3.8$ Hz, pyr-C), 131.10 (s, $-CH=CH-$), 103.55 (s, pyr-CH), 45.32 (s, Ir bound $-CH=CH-$), 37.05 (app. t, $J_{CP} = 3.8$ Hz, $-CH_2-CH_2-$), 32.93 (s, $-CH_2-CH_2-$), 26.81 (br s, $-CH_2-$), 25.31 (br s, $CH(CH_3)_2$), 19.26 (s, $CH(CH_3)_2$), 17.77 (s, $CH(CH_3)_2$). $^{31}P\{^1H\}$ NMR (162 MHz, C_6D_6): δ 44.31 (br s). The product **7** crystallizes from a concentrated dichloromethane solution layered with *n*-pentane as a dimer with loss of a molecule of COD to give $\{[(PN^{pyr}P)Ir]_2(COD)\}$ (**9**). For **9**: 1H (400 MHz, $23^\circ C$, C_6D_6): δ 6.55 (s, 4H, pyr-H), 3.50 (br s, 4H, $-CH=CH-$), 2.95 (d, $J_{HH} = 12.0$ Hz, 4H, $-CH_2-CH_2-$), 2.87 (br s, 8H, $-CH_2-P^iPr_2$), 2.02 (br s, 8H, $CH(CH_3)_2$), 1.79 (br s, 4H, $-CH_2-CH_2-$), 1.21 (br s, 24H, $CH(CH_3)_2$), 0.97 (app. quartet (dvt), 24H, $CH(CH_3)_2$). $^{13}C\{^1H\}$ NMR: (126 MHz, $23^\circ C$, C_6D_6): δ 140.19 (s, pyr-C), 103.61 (s, pyr-CH), 46.11 (s, $-CH=CH-$), 41.28 (s, $-CH_2-CH_2-$), 27–26 (br s, $-CH_2-$), 26–25 (br s, $CH(CH_3)_2$), 19.28 (br s, $CH(CH_3)_2$), 17.60 (s, $CH(CH_3)_2$). $^{31}P\{^1H\}$ NMR (162 MHz, $23^\circ C$, C_6D_6): δ 44.58 (br s), 43.72 (br s). 1H (400 MHz, $77^\circ C$, C_6D_6): δ 6.40 (s, 4H, pyr-H), 3.50 (br s, 4H, $-CH=CH-$), 2.90 (br s, 4H, $-CH_2-CH_2-$), 8H, $-CH_2-P^iPr_2$), 2.10 (m, 8H, $CH(CH_3)_2$), 1.75 (m, 4H, $-CH_2-CH_2-$), 1.21 (app. quartet (dvt), 24H, $CH(CH_3)_2$), 1.01 (app. quartet (dvt), 24H, $CH(CH_3)_2$). $^{13}C\{^1H\}$ NMR: (126 MHz, $77^\circ C$, C_6D_6): δ 140.03 (s, pyr-C), 103.62 (s, pyr-CH), 46.35 (s, $-CH=CH-$), 41.20 (s, $-CH_2-CH_2-$), 27.13 (app. t, $J_{CP} = 13$ Hz, $-CH_2-$), 25.60 (app. t, $J_{CP} = 13$ Hz, $CH(CH_3)_2$), 19.46 (s, $CH(CH_3)_2$), 17.80 (s, $CH(CH_3)_2$). $^{31}P\{^1H\}$ NMR (162 MHz, $77^\circ C$, C_6D_6): δ 44.55 (s). Anal. Calcd for $C_{44}H_{80}Ir_2N_2P_4$: C, 46.14; H, 7.04; N, 2.45. Found: 45.98; H, 7.25; N, 3.05.

Synthesis of $[(PN^{pyr}P)TI]$ (8**).** A vial containing $(PN^{pyr}P)H$ (**1**, 0.1162 g, 0.355 mmol) was stirred in toluene at $-78^\circ C$ for 15 min. A separate vial of nBuLi (1.6 M, 0.23 mL, 0.355 mmol) was diluted in toluene and also kept at low temperature for 15 min. At that time, the nBuLi solution was added dropwise to the cold $(PN^{pyr}P)H$ solution, stirred at low temperature for 15 min and then at room temperature for an hour, and toluene was removed under reduced pressure. Meanwhile, a tetrahydrofuran solution of TlOTf (0.125 g, 0.355 mmol, 5 mL) was cooled down to $-78^\circ C$. Once toluene was removed, $[(PN^{pyr}P)Li]$ was dissolved in 5 mL tetrahydrofuran and added, at low temperature, to the stirring TlOTf solution, which immediately turned black. The reaction was stirred for 15 min at low temperature and 30 min at room temperature. The volatiles were removed under reduced pressure and toluene was added to the reaction vial to precipitate LiOTf, and filtered to give a deep orange-brown solution. Volatiles were removed under reduced pressure and the crude residue was deep-orange in color (Yield = 0.180 g, 96%). Analytically pure **8** was isolated by recrystallization from a concentrated toluene solution. For **8**: 1H NMR: (500 MHz, C_6D_6): δ 6.30 (s, 2H, pyr-H), 3.06 (s, 4H, $-CH_2-$), 1.78 (m, 4H, $CH(CH_3)_2$), 1.07 (app. quartet (dvt), 12H, $CH(CH_3)_2$), 1.00 (app. quartet (dvt), 12H, $CH(CH_3)_2$). $^{13}C\{^1H\}$ NMR (100 MHz, C_6D_6): δ 136.56 (s, pyr-C), 107.43 (s, pyr-CH), 25.80 (app. t, $J_{CP} = 5.0$ Hz, $-CH_2-$), 24.47 (app. t, $J_{CP} = 6.0$ Hz, $CH(CH_3)_2$), 19.86 (app. t, $J_{CP} = 6.0$ Hz, $CH(CH_3)_2$). $^{31}P\{^1H\}$ NMR (162 MHz, C_6D_6): δ 39.31 (s). ^{205}Tl (285 MHz, C_6D_6): δ 3139.99 (s). Anal. Calcd for $C_{18}H_{34}NP_2Tl$: C, 40.73; H, 6.46; N, 2.64. Found: 39.84; H, 6.25; N, 3.32.

Synthesis of $[(PN^{pyr}P)Ir(COE)]$ (10**).** $[(PN^{pyr}P)TI]$ (0.0498 g, 0.0938 mmol) was dissolved in toluene and left stirring at $-78^\circ C$ for 20 min. $[Ir(COE)_2Cl]_2$ (0.0420 g, 0.0469 mmol) was weighed separately, dissolved in toluene, and added slowly to the $[(PN^{pyr}P)TI]$ solution at low temperature. The solution was stirred at low temperature for 20 min and room temperature for 25 min, when the solution changed from pale yellow to cloudy maroon. The reaction was filtered to give a dark precipitate and a deep red filtrate. Upon drying, a dark maroon product was obtained (yield = 0.0561 g, 95.0%). For **10**: 1H (500 MHz, $22^\circ C$, C_6D_6): δ 6.52 (s, 4H, pyr-H), 3.14 (m, 2H, $-CH=CH-$), 2.83 (s, 4H, $-CH_2-P^iPr_2$), 2.44 (m, 2H, $-CH_2-CH_2-$), 1.94–1.84 (m, 4H, $CH(CH_3)_2$), 2H, $-CH_2-CH_2-$), 1.75 (m, 2H, $-CH_2-CH_2-$), 1.64–1.45 (m, 6H, $-CH_2-CH_2-$), 1.11 (app. quartet (dvt), 12H, $CH(CH_3)_2$), 0.92 (app. quartet (dvt), 12H, $CH(CH_3)_2$). $^{13}C\{^1H\}$ NMR: (126 MHz, C_6D_6): δ 140.00 (s, pyr-C), 103.45 (s, pyr-CH), 44.61 (s, Ir bound $-CH=CH-$), 35.74 (app. t, $J_{CP} = 2.5$ Hz, $-CH_2-CH_2-$), 33.24 (s, $-CH_2-CH_2-$), 27.35 (s, $-CH_2-CH_2-$), 27.05 (br s, $-CH_2-$), 25.49 (br s, $-CH(CH_3)_2$), 19.23 (br s, $CH(CH_3)_2$), 17.71 (s, $CH(CH_3)_2$). $^{31}P\{^1H\}$ NMR (200 MHz, C_6D_6): δ 44.15 (br s), 43.67 (br s). Anal. Calcd for $C_{26}H_{48}IrNP_2$: C, 49.66; H, 7.69; N, 2.23. Found: 50.04; H, 7.60; N, 2.29.

Synthesis of $[(PN^{pyr}P)Ru(PPh_3)Cl]$ (11**).** **Method A, from $(PN^{pyr}P)H$ (**1**).** $(p\text{-cymene})RuCl_2$ (0.0561 g, 0.0916 mmol) and PPh_3 (0.0481 g, 0.183 mmol) were weighed, combined in a vial, dissolved in 5 mL tetrahydrofuran, and stirred for 2 h at room temperature. The initially clear, deep red solution became cloudy and a bright red-orange color within 10 min. At the same time, in a separate vial, $(PN^{pyr}P)H$ (**1**, 0.0625 g, 0.191 mmol) was dissolved in toluene and kept at $-78^\circ C$. After 2 h, the solution of **1** was added dropwise to the ruthenium solution at room temperature. No color change occurred. After 2 h of mixing time, the volatiles were removed under reduced pressure and a crude $^{31}P\{^1H\}$ NMR spectrum indicated that the desired product was not formed.

Method B, from $[(PN^{pyr}P)Li]$ (2**).** $(p\text{-cymene})RuCl_2$ (0.0656 g, 0.107 mmol) and PPh_3 (0.0562 g, 0.214 mmol) were weighed, combined in a vial, dissolved in 5 mL tetrahydrofuran, and stirred for 2 h at room temperature. The initially clear, deep red solution became cloudy and a brighter red-orange color within 10 min. At the same time, in a separate vial, $(PN^{pyr}P)H$ (**1**, 0.0730 g, 0.223 mmol) was dissolved in toluene and kept at $-78^\circ C$. After 15 min, nBuLi (1.6 M, 0.139 mL, 0.223 mmol) was added to the cold $(PN^{pyr}P)H$ solution, which was stirred at low temperature for 1.5 h and room temperature for 30 min. The $[(PN^{pyr}P)Li]$ solution was then added dropwise to the

stirring ruthenium solution at room temperature, changing from bright cloudy red-orange to a clear maroon-brown solution within 5 min. After 2 h, there was no other visible change, the volatiles were removed under reduced pressure and a $^{31}\text{P}\{^1\text{H}\}$ NMR spectrum taken. Its integration indicated that the desired product was formed in 26% yield, $(\text{PN}^{\text{pyr}}\text{P})\text{H}$ and PPh_3 accounted for 44% of the products, and many other side products for the remaining 30%.

Method C, from $[(\text{PN}^{\text{pyr}}\text{P})\text{TI}]$ (8). In a 50 mL Schlenk tube, PPh_3 (0.0386, 0.147 mmol) and $[(p\text{-cymene})\text{RuCl}_2]_2$ (0.0451 g, 0.0737 mmol) were dissolved in a small amount of C_6H_6 and heated at 65°C for 2 h to form a cloudy bright red solution. At this point, $[(\text{PN}^{\text{pyr}}\text{P})\text{TI}]$ (8, 0.0815 g, 0.153 mmol) was dissolved in C_6H_6 and added to the red solution. The Schlenk flask was heated for an additional 2 h at 65°C . Within minutes, the solution started to become darker and turned to brown, and within 10 min became a deep green color with an obvious white precipitate (TlCl). Once this color persisted for over an hour, the reaction was transferred to a vial, the volatiles removed, and the reaction triturated with *n*-pentane. Et_2O was added to the dark green precipitate and the resulting solution was filtered to give an orange-green filtrate (*p*-cymene) and a deep green precipitate (product). The solid was extracted in C_6H_6 and the resulting solution filtered through Celite to give a dark solid (yield = 0.1052 g, 94.5%).

Method D, from $[(\text{PN}^{\text{pyr}}\text{P})\text{Ag}]_2$ (12). $[(p\text{-cymene})\text{RuCl}_2]_2$ (0.0320 g, 0.0523 mmol) and PPh_3 (0.0249 g, 0.0950 mmol) were combined in 5 mL tetrahydrofuran and stirred at room temperature for 2 h, starting as a clear red solution and becoming a cloudy red/orange solution after 20 min. $[(\text{PN}^{\text{pyr}}\text{P})\text{Ag}]_2$ (12, 0.0411 g, 0.0473 mmol) was then separately dissolved in 5 mL tetrahydrofuran and added slowly to the stirring ruthenium solution, at which point the solution became lighter, more clear, and more brown in color. After 1.5 h, the volatiles were removed under reduced pressure, toluene was added to aid the precipitation of AgCl , and the solution was allowed to stir for an additional 2.5 h. At this point, the cloudy solution was filtered, giving a deep brown solution and a small amount of a brown precipitate. The desired product was obtained from the toluene filtrate upon removal of the volatiles, and identified by $^{31}\text{P}\{^1\text{H}\}$ NMR spectroscopy (24.5%) among some starting material (13.9%) and other products (61.6%); its isolation was not attempted. For **11**: ^1H NMR: (500 MHz, C_6D_6): δ 7.55 (m, 6H, $\text{P}(\text{C}_6\text{H}_5)_3$), 6.95 (m, 9H, $\text{P}(\text{C}_6\text{H}_5)_3$), 6.47 (s, 2H, pyr-H), 2.94 (app. dt, 2H, $^2J_{\text{HH}} = 15.0$ Hz, $J_{\text{HP}} = 5.0$ Hz, $-\text{CH}_2-$), 2.32 (m, 2H, $\text{CH}(\text{CH}_3)_2$), 1.96 (d, $^2J_{\text{HH}} = 15.0$ Hz, $-\text{CH}_2-$), 1.44 (app. quartet (dvt), 6H, $\text{CH}(\text{CH}_3)_2$), 1.32 (m, 2H, $\text{CH}(\text{CH}_3)_2$) 1.10 (app. quartet (dvt), 6H, $\text{CH}(\text{CH}_3)_2$), 0.97 (app. quartet (dvt), 6H, $\text{CH}(\text{CH}_3)_2$), 0.78 (app. quartet (dvt), 6H, $\text{CH}(\text{CH}_3)_2$). $^{13}\text{C}\{^1\text{H}\}$ NMR: (126 MHz, CDCl_3): δ 137.84 (dt, $^1J_{\text{CP}} = 13.9$ Hz, $^3J_{\text{CP}} = 3.8$ Hz, $\text{P}(\text{C}_6\text{H}_5)_3$), 137.39 (app. t, $J_{\text{CP}} = 3.8$ Hz, pyr-C), 134.77 (d, $J_{\text{CP}} = 10.1$ Hz, $\text{P}(\text{C}_6\text{H}_5)_3$), 129.26 (d, $J_{\text{CP}} = 3.2$ Hz, $\text{P}(\text{C}_6\text{H}_5)_3$), 127.62 (d, $J_{\text{CP}} = 6.3$ Hz, $\text{P}(\text{C}_6\text{H}_5)_3$), 106.59 (app. t, $J_{\text{CP}} = 5.0$ Hz, pyr-CH), 27.88 (app. t, $J_{\text{CP}} = 10.1$ Hz, $-\text{CH}_2-$), 25.91 (app. t, $J_{\text{CP}} = 8.8$ Hz, $\text{CH}(\text{CH}_3)_2$), 25.80 (app. t, $J_{\text{CP}} = 8.8$ Hz, $\text{CH}(\text{CH}_3)_2$), 20.91 (s, $\text{CH}(\text{CH}_3)_2$), 20.45 (s, $\text{CH}(\text{CH}_3)_2$), 20.11 (s, $\text{CH}(\text{CH}_3)_2$), 18.21 (s, $\text{CH}(\text{CH}_3)_2$). $^{31}\text{P}\{^1\text{H}\}$ NMR (200 MHz, C_6D_6): δ 87.67 (t, $^2J_{\text{PP}} = 30.0$ Hz), 48.69 (d, $^2J_{\text{PP}} = 30.0$ Hz). Anal. Calcd for $\text{C}_{36}\text{H}_{49}\text{ClNP}_3\text{Ru}$: C, 59.62; H, 6.81; N 1.93. Found: C, 59.55; H, 6.70; N 1.84.

Synthesis of $[(\text{PN}^{\text{pyr}}\text{P})\text{Ag}]_2$ (12). **Method A.** In a 20 mL scintillation vial wrapped in aluminum foil, $(\text{PN}^{\text{pyr}}\text{P})\text{H}$ (1, 0.0397 g, 0.121 mmol) was weighed and dissolved in Et_2O . AgPF_6 (0.0368, 0.146 mmol) was weighed in a separate, foiled vial and added to the former solution. The reaction became a cloudy, off-white solution. KO^tBu was weighed (0.0163 g, 0.146 mmol) and added to the reaction vial. The solution gradually darkened and became deep brown, indicating that the reaction is nearly complete. After about 2 h, the solution was filtered to give a rusty-orange clear solution. Once volatiles were removed, $[(\text{PN}^{\text{pyr}}\text{P})\text{Ag}]_2$ was obtained as a tan solid (yield = 0.0472 g, 89.9%).

Method B. In a 20 mL scintillation vial wrapped in aluminum foil, $(\text{PN}^{\text{pyr}}\text{P})\text{H}$ (1, 0.1575 g, 0.481 mmol) was weighed and dissolved in Et_2O . Ag_2O (0.0613, 0.265 mmol) was weighed in a separate, foiled vial and added to the former solution. After 18 h, the solution

transformed from cloudy black (undissolved Ag_2O) to cloudy olive green. The solution was filtered to give an orange-brown clear solution. Once volatiles were removed, $[(\text{PN}^{\text{pyr}}\text{P})\text{Ag}]_2$ was obtained (yield = 0.1357 g, 65.2%). For **12**: ^1H NMR: (500 MHz, C_6D_6): δ 6.35 (s, 2H, pyr-H), 3.15 (s, 4H, $-\text{CH}_2-$), 1.75 (m, 4H, CHMe_2), 1.04 (app. quartet (dvt), 12H, $\text{CH}(\text{CH}_3)_2$), 0.99 (app. quartet (dvt), 12H, $\text{CH}(\text{CH}_3)_2$). $^{13}\text{C}\{^1\text{H}\}$ NMR (126 MHz, C_6D_6): δ 131.86 (s, pyr-C), 106.31 (s, pyr-CH), 26.12 (s, $-\text{CH}_2-$), 24.02 (s, $\text{CH}(\text{CH}_3)_2$), 19.84 (s, $\text{CH}(\text{CH}_3)_2$), 19.09 (s, $\text{CH}(\text{CH}_3)_2$). $^{31}\text{P}\{^1\text{H}\}$ NMR (200 MHz, C_6D_6): δ 19.93 (d, $^1J_{107\text{Ag-P}} = 394$ Hz, d, $^1J_{109\text{Ag-P}} = 454$ Hz). Anal. Calcd for $\text{C}_{36}\text{H}_{68}\text{Ag}_2\text{N}_2\text{P}_4$: C, 49.78; H, 7.89; N 3.23. Found: C, 50.42; H, 8.10; N 3.17.

X-ray crystal structure of $[(\text{PN}^{\text{pyr}}\text{P})\text{H}(\text{Ir}(\text{COD})\text{Cl})_2]$ (2). Bright orange crystals were grown in 5 days from a concentrated solution of dichloromethane layered with hexanes at -34°C in the glovebox. Crystal and refinement data for **2**: $\text{C}_{34}\text{H}_{59}\text{Cl}_2\text{Ir}_2\text{NP}_2$; $M_r = 999.06$; Monoclinic; space group $\text{P}2(1)/n$; $a = 15.6504(17)$ Å; $b = 12.9926(14)$ Å; $c = 17.5170(18)$ Å; $\alpha = 90^\circ$; $\beta = 97.8616(18)^\circ$; $\gamma = 90^\circ$; $V = 3528.4(7)$ Å³; $Z = 4$; $T = 120(2)$ K; $\lambda = 0.71073$ Å; $\mu = 7.802$ mm⁻¹; $d_{\text{calc}} = 1.881$ g·cm⁻³; 35822 reflections collected; 6210 unique ($R_{\text{int}} = 0.0789$); giving $R_1 = 0.0338$, $wR_2 = 0.0556$ for 4849 data with $[I > 2\sigma(I)]$ and $R_1 = 0.0557$, $wR_2 = 0.0588$ for all 6210 data. Residual electron density ($\text{e}^- \cdot \text{Å}^{-3}$) max/min: 1.441/−1.186.

X-ray crystal structure of $[(\text{PN}^{\text{pyr}}\text{P})\text{NiCl}]$ (4). Single crystals were obtained as thin, bright orange plates from a solution of dichloromethane layered with pentane at -34°C in the glovebox. Crystal and refinement data for **4**: $\text{C}_{18}\text{H}_{34}\text{ClNP}_2\text{Ni}$; $M_r = 420.56$; Triclinic; space group $\text{P}-1$; $a = 10.8266(15)$ Å; $b = 13.6723(19)$ Å; $c = 14.637(2)$ Å; $\alpha = 77.549(3)^\circ$; $\beta = 83.824(3)^\circ$; $\gamma = 89.904(2)^\circ$; $V = 2102.9(5)$ Å³; $Z = 4$; $T = 120(2)$ K; $\lambda = 0.71073$ Å; $\mu = 1.201$ mm⁻¹; $d_{\text{calc}} = 1.328$ g·cm⁻³; 32410 reflections collected; 7416 unique ($R_{\text{int}} = 0.0767$); giving $R_1 = 0.0414$, $wR_2 = 0.0637$ for 5126 data with $[I > 2\sigma(I)]$ and $R_1 = 0.0764$, $wR_2 = 0.0685$ for all 7416 data. Residual electron density ($\text{e}^- \cdot \text{Å}^{-3}$) max/min: 0.466/−0.471.

X-ray crystal structure of $[(\text{PN}^{\text{pyr}}\text{P})\text{PtCl}]$ (6). Single crystals were obtained as thin, pale orange plates from a solution of concentrated diethyl ether with dichloromethane at -34°C in the glovebox. Crystal and refinement data for **6**: $\text{C}_{18}\text{H}_{34}\text{ClNP}_2\text{Pt}$; $M_r = 556.94$; Triclinic; space group $\text{P}-1$; $a = 10.9420(8)$ Å; $b = 13.7285(10)$ Å; $c = 14.5082(11)$ Å; $\alpha = 77.757(3)^\circ$; $\beta = 82.949(3)^\circ$; $\gamma = 89.707(3)^\circ$; $V = 2113.2(3)$ Å³; $Z = 4$; $T = 120(2)$ K; $\lambda = 0.71073$ Å; $\mu = 6.918$ mm⁻¹; $d_{\text{calc}} = 1.751$ g·cm⁻³; 37383 reflections collected; 7423 unique ($R_{\text{int}} = 0.0530$); giving $R_1 = 0.0282$, $wR_2 = 0.0520$ for 5007 data with $[I > 2\sigma(I)]$ and $R_1 = 0.0575$, $wR_2 = 0.0574$ for all 7423 data. Residual electron density ($\text{e}^- \cdot \text{Å}^{-3}$) max/min: 1.206/−1.480.

X-ray crystal structure of $[(\text{PN}^{\text{pyr}}\text{P})\text{TI}]$ (8). Crystals were grown from a concentrated tetrahydrofuran solution over 2 days at -34°C in the glovebox and appeared as large, colorless blocks. Crystal and refinement data for **8**: $\text{C}_{18}\text{H}_{34}\text{NP}_2\text{TI}$; $M_r = 530.77$; Orthorhombic; space group $\text{P}2(1)2(1)2(1)$; $a = 9.4029(3)$ Å; $b = 13.8251(4)$ Å; $c = 16.2702(5)$ Å; $\alpha = 90^\circ$; $\beta = 90^\circ$; $\gamma = 90^\circ$; $V = 2115.06(11)$ Å³; $Z = 4$; $T = 120(2)$ K; $\lambda = 0.71073$ Å; $\mu = 7.786$ mm⁻¹; $d_{\text{calc}} = 1.667$ g·cm⁻³; 29287 reflections collected; 3727 unique ($R_{\text{int}} = 0.0371$); giving $R_1 = 0.0145$, $wR_2 = 0.0292$ for 3628 data with $[I > 2\sigma(I)]$ and $R_1 = 0.0156$, $wR_2 = 0.0297$ for all 3727 data. Residual electron density ($\text{e}^- \cdot \text{Å}^{-3}$) max/min: 0.650/−0.300.

X-ray crystal structure of $[(\text{PN}^{\text{pyr}}\text{P})\text{Ir}]_2(\text{COD})$ (9·2CH₂Cl₂). Orange crystals suitable for single X-ray diffraction were grown from a concentrated solution of dichloromethane layered with hexanes at -34°C in the glovebox. Crystal and refinement data for **9·2CH₂Cl₂**: $\text{C}_{48}\text{H}_{88}\text{Cl}_8\text{Ir}_2\text{N}_2\text{P}_4$; $M_r = 1485.08$; Monoclinic; space group $\text{P}2(1)/c$; $a = 13.6618(12)$ Å; $b = 16.8234(15)$ Å; $c = 13.9669(13)$ Å; $\alpha = 90^\circ$; $\beta = 111.412(2)^\circ$; $\gamma = 90^\circ$; $V = 2988.6(5)$ Å³; $Z = 2$; $T = 120(2)$ K; $\lambda = 0.71073$ Å; $\mu = 4.946$ mm⁻¹; $d_{\text{calc}} = 1.650$ g·cm⁻³; 25834 reflections collected; 5266 unique ($R_{\text{int}} = 0.0690$); giving $R_1 = 0.0362$, $wR_2 = 0.0738$ for 3968 data with $[I > 2\sigma(I)]$ and $R_1 = 0.0604$, $wR_2 = 0.0789$ for all 5266 data. Residual electron density ($\text{e}^- \cdot \text{Å}^{-3}$) max/min: 3.094/−1.065.

X-ray crystal structure of $[(\text{PN}^{\text{pyr}}\text{P})\text{Ru}(\text{PPh}_3)\text{Cl}]$ (11). Single crystals (dichroic, forest green/rusty orange) were grown from a

concentrated toluene solution at $-34\text{ }^{\circ}\text{C}$ in the glovebox. Crystal and refinement data for **11**: $\text{C}_{36}\text{H}_{49}\text{ClNP}_3\text{Ru}$; $M_r = 725.19$; Triclinic; space group P-1; $a = 10.6389(8)\text{ \AA}$; $b = 10.8343(7)\text{ \AA}$; $c = 17.2221(13)\text{ \AA}$; $\alpha = 72.0094(15)^{\circ}$; $\beta = 80.9480(17)^{\circ}$; $\gamma = 65.8789(14)^{\circ}$; $V = 1722.1(2)\text{ \AA}^3$; $Z = 2$; $T = 120(2)\text{ K}$; $\lambda = 0.71073\text{ \AA}$; $\mu = 0.698\text{ mm}^{-1}$; $d_{\text{calc}} = 1.399\text{ g}\cdot\text{cm}^{-3}$; 24274 reflections collected; 6065 unique ($R_{\text{int}} = 0.0309$); giving $R_1 = 0.0462$, $wR_2 = 0.1126$ for 5185 data with $[I > 2\sigma(I)]$ and $R_1 = 0.0569$, $wR_2 = 0.1182$ for all 6065 data. Residual electron density ($\text{e}^{-}\cdot\text{\AA}^{-3}$) max/min: 1.633/−1.470.

X-ray crystal structure of [(PN^{py}P)Ag]₂ (12). Single crystals were obtained as colorless, thin plates from a concentrated solution of diethyl ether layered with pentane at $-34\text{ }^{\circ}\text{C}$ in the glovebox. Crystal and refinement data for **12**: Crystal data for $\text{C}_{36}\text{H}_{68}\text{Ag}_2\text{N}_2\text{P}_4$; $M_r = 868.54$; Orthorhombic; space group P2(1)2(1)2(1); $a = 11.6741(8)\text{ \AA}$; $b = 12.4087(8)\text{ \AA}$; $c = 28.6835(18)\text{ \AA}$; $\alpha = 90^{\circ}$; $\beta = 90^{\circ}$; $\gamma = 90^{\circ}$; $V = 4155.1(5)\text{ \AA}^3$; $Z = 4$; $T = 120(2)\text{ K}$; $\lambda = 0.71073\text{ \AA}$; $\mu = 1.122\text{ mm}^{-1}$; $d_{\text{calc}} = 1.388\text{ g}\cdot\text{cm}^{-3}$; 69422 reflections collected; 8147 unique ($R_{\text{int}} = 0.0903$); giving $R_1 = 0.0378$, $wR_2 = 0.0730$ for 7116 data with $[I > 2\sigma(I)]$ and $R_1 = 0.0487$, $wR_2 = 0.0768$ for all 8147 data. Residual electron density ($\text{e}^{-}\cdot\text{\AA}^{-3}$) max/min: 0.864/−0.808.

■ ASSOCIATED CONTENT

■ Supporting Information

NMR spectra for compounds **1–12**; crystallographic tables and details (CIF) for compounds **2, 4, 6, 8, 9, 11, and 12**; complete ref 68; and a text file of all computed Cartesian coordinates in a format for convenient visualization. This material is available free of charge via the Internet at <http://pubs.acs.org>.

■ AUTHOR INFORMATION

Corresponding Author

*E-mail: viluc@nd.edu.

Notes

The authors declare no competing financial interest.

■ ACKNOWLEDGMENTS

We gratefully acknowledge Seth N. Brown for discussions and suggestions and Allen Oliver for crystallographic assistance. This work was supported by the University of Notre Dame, by Donors of the American Chemical Society Petroleum Research Fund (ACS PRF # 53536-DNI3), and by an Arthur J. Schmitt Fellowship to J.A.K.

■ REFERENCES

- (1) Albrecht, M.; van Koten, G. *Angew. Chem., Int. Ed.* **2001**, *40*, 3750.
- (2) Gelman, D.; Romm, R. In *Organometallic Pincer Chemistry*; van Koten, G., Milstein, D., Eds.; Springer: Berlin Heidelberg, 2013; Vol. 40, p 289.
- (3) Szabó, K. In *Organometallic Pincer Chemistry*; van Koten, G., Milstein, D., Eds.; Springer: Berlin Heidelberg, 2013; Vol. 40, p 203.
- (4) Roddick, D. In *Organometallic Pincer Chemistry*; van Koten, G., Milstein, D., Eds.; Springer: Berlin Heidelberg, 2013; Vol. 40, p 49.
- (5) Schneider, S.; Meiners, J.; Askevold, B. *Eur. J. Inorg. Chem.* **2012**, *2012*, 412.
- (6) van der Boom, M. E.; Milstein, D. *Chem. Rev.* **2003**, *103*, 1759.
- (7) Gunanathan, C.; Milstein, D. *Acc. Chem. Res.* **2011**, *44*, 588.
- (8) van der Vlugt, J. I.; Reek, J. N. H. *Angew. Chem., Int. Ed.* **2009**, *48*, 8832.
- (9) Milstein, D. *Top. Catal.* **2010**, *53*, 915.
- (10) Mashima, K.; Tsunugi, H. *J. Organomet. Chem.* **2005**, *690*, 4414.
- (11) Tian, R.; Ng, Y.; Ganguly, R.; Mathey, F. *Organometallics* **2012**, *31*, 2486.
- (12) Lien, Y.-L.; Chang, Y.-C.; Chuang, N.-T.; Datta, A.; Chen, S.-J.; Hu, C.-H.; Huang, W.-Y.; Lin, C.-H.; Huang, J.-H. *Inorg. Chem.* **2009**, *49*, 136.

- (13) Hsu, J.-W.; Lin, Y.-C.; Hsiao, C.-S.; Datta, A.; Lin, C.-H.; Huang, J.-H.; Tsai, J.-C.; Hsu, W.-C. *Dalton Trans.* **2012**, *41*, 7700.
- (14) Wang, Y.-T.; Lin, Y.-C.; Hsu, S.-Y.; Chen, R.-Y.; Liu, P.-H.; Datta, A.; Lin, C.-H.; Huang, J.-H. *J. Organomet. Chem.* **2013**, *745–746*, 12.
- (15) Li, R.; Larsen, D. S.; Brooker, S. *New J. Chem.* **2003**, *27*, 1353.
- (16) Ghorai, D.; Kumar, S.; Mani, G. *Dalton Trans.* **2012**, *41*, 9503.
- (17) Maaß, C.; Andrada, D. M.; Mata, R. A.; Herbst-Irmer, R.; Stalke, D. *Inorg. Chem.* **2013**, *52*, 9539.
- (18) Mazet, C.; Gade, L. H. *Organometallics* **2001**, *20*, 4144.
- (19) Mazet, C.; Gade, L. H. *Chem.—Eur. J.* **2003**, *9*, 1759.
- (20) Mazet, C.; Gade, Lutz H. *Eur. J. Inorg. Chem.* **2003**, *2003*, 1161.
- (21) Gruger, N.; Wadepohl, H.; Gade, L. H. *Dalton Trans.* **2012**, *41*, 14028.
- (22) Kumar, S.; Mani, G.; Mondal, S.; Chattaraj, P. K. *Inorg. Chem.* **2012**, *51*, 12527.
- (23) Venkanna, G. T.; Ramos, T. V. M.; Arman, H. D.; Tonzetich, Z. *J. Inorg. Chem.* **2012**, *51*, 12789.
- (24) Venkanna, G. T.; Tammineni, S.; Arman, H. D.; Tonzetich, Z. *J. Organometallics* **2013**, *32*, 4656.
- (25) Naota, T.; Takaya, H.; Murahashi, S.-I. *Chem. Rev.* **1998**, *98*, 2599.
- (26) Trost, B. M.; Toste, F. D.; Pinkerton, A. B. *Chem. Rev.* **2001**, *101*, 2067.
- (27) Arockiam, P. B.; Bruneau, C.; Dixneuf, P. H. *Chem. Rev.* **2012**, *112*, 5879.
- (28) Crabtree, R. In *Iridium Catalysis*; Andersson, P. G., Ed.; Springer: Berlin Heidelberg, 2011; Vol. 34, p 1.
- (29) Cadu, A.; Andersson, P. G. *Dalton Trans.* **2013**, *42*, 14345.
- (30) Choi, J.; MacArthur, A. H. R.; Brookhart, M.; Goldman, A. S. *Chem. Rev.* **2011**, *111*, 1761.
- (31) Jensen, C. M. *Chem. Commun.* **1999**, 2443.
- (32) Goldman Alan, S.; Renkema Kenton, B.; Czerw, M.; Krogh-Jespersen, K. In *Activation and Functionalization of C-H Bonds*; American Chemical Society: 2004; Vol. 885, p 198.
- (33) Albrecht, M.; Morales-Morales, D. In *Iridium Complexes in Organic Synthesis*; Wiley-VCH Verlag GmbH & Co. KGaA: 2009; p 299.
- (34) Ozerov, O. V.; Guo, C.; Papkov, V. A.; Foxman, B. M. *J. Am. Chem. Soc.* **2004**, *126*, 4792.
- (35) Haibach, M. C.; Wang, D. Y.; Emge, T. J.; Krogh-Jespersen, K.; Goldman, A. S. *Chem. Sci.* **2013**, *4*, 3683.
- (36) Hitchcock, P. B.; Lappert, M. F.; Leung, W.-P.; Yin, P. *J. Chem. Soc., Dalton Trans.* **1995**, 3925.
- (37) Colquhoun, I. J.; McFarlane, H. C. E.; McFarlane, W. J. *Chem. Soc., Chem. Commun.* **1982**, 220.
- (38) Hitchcock, P. B.; Lappert, M. F.; Power, P. P.; Smith, S. J. *J. Chem. Soc., Chem. Commun.* **1984**, 1669.
- (39) Reich, H. J.; Dykstra, R. R. *Organometallics* **1994**, *13*, 4578.
- (40) Fryzuk, M. D.; MacNeil, P. A.; Rettig, S. J.; Secco, A. S.; Trotter, J. *Organometallics* **1982**, *1*, 918.
- (41) DeMott, J. C.; Basuli, F.; Kilgore, U. J.; Foxman, B. M.; Huffman, J. C.; Ozerov, O. V.; Míndiola, D. J. *Inorg. Chem.* **2007**, *46*, 6271.
- (42) Peters, J. C.; Harkins, S. B.; Brown, S. D.; Day, M. W. *Inorg. Chem.* **2001**, *40*, 5083.
- (43) Gade, L. H. *Dalton Trans.* **2003**, 267.
- (44) Shapiro, I. R.; Jenkins, D. M.; Thomas, J. C.; Day, M. W.; Peters, J. C. *Chem. Commun.* **2001**, 2152.
- (45) Betley, T. A.; Peters, J. C. *Inorg. Chem.* **2003**, *42*, 5074.
- (46) Arenas, I.; Fuentes, M. Á.; Álvarez, E.; Díaz, Y.; Caballero, A.; Castellón, S.; Pérez, P. J. *Inorg. Chem.* **2014**, *53*, 3991.
- (47) Bondi, A. *J. Phys. Chem.* **1964**, *68*, 441.
- (48) Cordero, B.; Gomez, V.; Platero-Prats, A. E.; Reves, M.; Echeverria, J.; Cremades, E.; Barragan, F.; Alvarez, S. *Dalton Trans.* **2008**, 2832.
- (49) Thomas, J. C.; Peters, J. C. *Inorg. Chem.* **2003**, *42*, 5055.
- (50) Dubs, C.; Yamamoto, T.; Inagaki, A.; Akita, M. *Organometallics* **2006**, *25*, 1359.

- (51) Graeupner, J.; Brewster, T. P.; Blakemore, J. D.; Schley, N. D.; Thomsen, J. M.; Brudvig, G. W.; Hazari, N.; Crabtree, R. H. *Organometallics* **2012**, *31*, 7158.
- (52) Calimano, E.; Tilley, T. D. *J. Am. Chem. Soc.* **2009**, *131*, 11161.
- (53) Ben-Ari, E.; Leitun, G.; Shimon, L. J. W.; Milstein, D. *J. Am. Chem. Soc.* **2006**, *128*, 15390.
- (54) Guo, L.; Liu, Y.; Yao, W.; Leng, X.; Huang, Z. *Org. Lett.* **2013**, *15*, 1144.
- (55) Whited, M. T.; Zhu, Y.; Timpa, S. D.; Chen, C.-H.; Foxman, B. M.; Ozerov, O. V.; Grubbs, R. H. *Organometallics* **2009**, *28*, 4560.
- (56) Friedrich, A.; Ghosh, R.; Kolb, R.; Herdtweck, E.; Schneider, S. *Organometallics* **2009**, *28*, 708.
- (57) Michlik, S.; Kempe, R. *Nat. Chem.* **2013**, *5*, 140.
- (58) Serron, S. A.; Nolan, S. P. *Organometallics* **1995**, *14*, 4611.
- (59) Medici, S.; Gagliardo, M.; Williams, S. B.; Chase, P. A.; Gladiali, S.; Lutz, M.; Spek, A. L.; van Klink, G. P. M.; van Koten, G. *Helv. Chim. Acta* **2005**, *88*, 694.
- (60) Jia, G.; Lee, H. M.; Williams, I. D. *J. Organomet. Chem.* **1997**, *534*, 173.
- (61) Jia, G.; Lee, H. M.; Xia, H. P.; Williams, I. D. *Organometallics* **1996**, *15*, 5453.
- (62) Amoroso, D.; Jabri, A.; Yap, G. P. A.; Gusev, D. G.; dos Santos, E. N.; Fogg, D. E. *Organometallics* **2004**, *23*, 4047.
- (63) Ren, P.; Vechorkin, O.; Csok, Z.; Salihu, I.; Scopelliti, R.; Hu, X. *Dalton Trans.* **2011**, *40*, 8906.
- (64) Gagliardo, M.; Chase, P. A.; Lutz, M.; Spek, A. L.; Hartl, F.; Havenith, R. W. A.; van Klink, G. P. M.; van Koten, G. *Organometallics* **2005**, *24*, 4553.
- (65) Tseng, K.-N. T.; Kampf, J. W.; Szymczak, N. K. *Organometallics* **2013**, *32*, 2046.
- (66) Zhang, J.; Gandelman, M.; Shimon, L. J. W.; Milstein, D. *Dalton Trans.* **2007**, 107.
- (67) van der Vlugt, J. I.; Siegler, M. A.; Janssen, M.; Vogt, D.; Spek, A. L. *Organometallics* **2009**, *28*, 7025.
- (68) Kim, I. T.; Elsenbaumer, R. L. *Tetrahedron Lett.* **1998**, *39*, 1087.
- (69) Frisch, M. J. In *Gaussian 03, revision D.02*; Gaussian, Inc.: Wallingford CT, 2004.